1   **Resilience of Phytoplankton Dynamics to Trophic Cascades and Nutrient Enrichment**

2   paper for *Limnology & Oceanography* special issue on resilience

3

4

5

6   Stephen R. Carpenter*[1], Babak M.S. Arani[2], Egbert H. Van Nes[2], Marten Scheffer[2],

7   Michael L. Pace[3]

8

9   [1] Center for Limnology, University of Wisconsin, Madison, WI 53706 U.S.A.

10

11   [2] Aquatic Ecology and Water Quality Management, Wageningen University, P.O. Box 47, 6700

12   AA Wageningen, The Netherlands

13

14   [3] Department of Environmental Sciences, University of Virginia, Charlottesville, Virginia 22904

15   U.S.A.

16

17   *Correspondence: Steve.Carpenter@wisc.edu

18

19   **Running Head:** Resilience and Randomness

Abstract

Resilience was compared for alternate states of phytoplankton pigment concentration in two multi-year whole-lake experiments designed to shift the manipulated ecosystem between alternate states. Mean exit time, the average time between threshold crossings, was calculated from automated measurements every 5 minutes during summer stratification. Alternate states were clearly identified, and equilibria showed narrow variation in bootstrap analysis of uncertainty. Mean exit times ranged from 13 to 290 hours. In the reference ecosystem, Paul Lake, mean exit time of the low-pigment state was about 100 hours longer than mean exit time of the high-pigment state. In the manipulated ecosystem, Peter Lake, mean exit time of the high-pigment state exceeded that of the low-pigment state by 30 hours in the Cascade experiment. In the enrichment experiment mean exit time of the low-pigment state was longer than that of the high-pigment state by about 100 hours. Mean exit time is a useful measure of resilience for stochastic ecosystems where high-frequency measurements are made by consistent methods over the full range of ecosystem states.

Scientific Significance Statement Topic

A novel indicator of resilience, mean exit time, accounts for the natural variability of ecosystems. We estimated mean exit times for low- and high-pigment states of lakes in experiments that gradually shifted the ecosystems between states by two different mechanisms, trophic cascades and nutrient enrichments. Mean exit times of the manipulated lake were

2

46 substantially different from those of the unmanipulated reference lake. It is useful to account for

47 the high variability of phytoplankton biomass as lakes shift among alternate states.

48

49 **Scientific Significance Statement Outlet**

50

51 The paper introduces a novel indicator of resilience, mean exit time, that includes the role of

52 randomness in resilience. We demonstrate the application of mean exit time using two whole-

53 lake experiments that were designed to investigate alternate states caused by enrichment and

54 trophic cascades.

55

56 **Data Availability**

57

58 Data used here are downloadable from:

59

60 Carpenter, S., M. Pace, J. Cole, R. Batt, C. Buelo, and J. Kurzweil. 2018. Cascade Project at

61 North Temperate Lakes LTER High Frequency Sonde Data from Food Web Resilience

62 Experiment 2008 - 2011 ver 1. Environmental Data Initiative.

63 https://doi.org/10.6073/pasta/5a8c6398661fad0bc8f1f5119b1150d6

64

65 Pace, M., J. Cole, and S. Carpenter. 2020. Cascade project at North Temperate Lakes LTER -

66 High Frequency Data for Whole Lake Nutrient Additions 2013-2015 ver 2. Environmental Data

67 Initiative. https://doi.org/10.6073/pasta/cbe19041db41e720d84970f43156c042.

68

69 Lake ecosystems provide diverse examples of complex dynamics, including multiple stable

70 states and critical transitions among them (Scheffer 1998; Scheffer 2009). These include

71 alternate states of phytoplankton biomass resulting from either trophic cascades or nutrient

72 enrichment (Carpenter 2003).

73

74 Holling (Holling 1973a) recognized that ecosystems exhibit multiple states and occasionally shift

75 among them. Holling introduced *resilience* as "the persistence of relationships within a system"

76 and "a measure of the ability of these systems to absorb changes of state variables, driving

77 variables, and parameters, and still persist". He distinguished resilience from *stability*, "the

78 ability of a system to return to an equilibrium state after a temporary disturbance". Unlike

79 stability which is a local measure that treats perturbations as isolated events, resilience accounts

80 for perturbations of large amplitudes and the ongoing tempo of sequential disturbances. A

81 section titled "The Random World" (p 13-15 of Holling 1973) discusses the role of random

82 fluctuations in resilience, including examples from lake eutrophication, food webs, and fisheries.

83 Holling's ideas of resilience imply probabilities of persistence of an ecosystem state or identity

84 in a stochastic environment. However most research has focused on deterministic aspects of

85 resilience and few quantitative studies have addressed resilience in a stochastic framework.

86

87 Arani et al. (2021) proposed 'exit time' as a stochastic measure of resilience. Exit time, a

88 stochastic variable, is the average time until a shift between states of a stochastic system is first

89 observed. The mean exit time, or the median, can serve as a resilience measure. A familiar

90 example is half-life of a radioisotope. Decay from the radioactive state to the daughter state is a

91 stochastic process of single atoms. Its half-life is the median exit time, or time until half of the

92   radioactive atoms have decayed. In global change science, Kleinen et al. (2003) mentioned exit

93   time from Atlantic Meridional Overturning Circulation (AMOC, the state of the ocean that

94   brings a mild climate to Western Europe) as a measure of the expected time available for policy

95   action to maintain resilience of Europe's climate. Arani et al. (2021) present empirical methods

96   for measuring exit time from ecosystem states using time series data. We apply that method here

97   to assess resilience of experimental lakes to trophic cascades and nutrient enrichment.

98

99   In 2008 we began a series of experiments designed to gradually shift lake ecosystems between

100   alternate states. Our goal was to evaluate dynamic indicators of resilience based on statistical

101   changes in time series as the lake shifted from one state to another (Carpenter et al. 2011; Pace et

102   al. 2017; Scheffer et al. 2015; Wilkinson et al. 2018). Because these studies measured lake

103   ecosystem variables frequently during both states of the ecosystem and the transition, the data

104   are suitable for estimating exit time. Here, we determine mean exit times for two different

105   manipulations that induced alternate states and provided high-frequency time series needed to

106   assess exit time as a quantitative measure of resilience as described by Holling (1973).

107

108   ***Methods***

109

110   **Peter and Paul Lakes**

111

112   Paul and Peter lakes are paired lakes in Gogebic County, Michigan, USA (46°250 N, 89°500 W).

113   Since 1951 the lakes have been used for whole-lake experiments with Paul as the reference lake

114   and Peter as the manipulated lake (Elser et al. 1986). Since 1984 the lakes have been used for a

series of experiments on trophic cascades, allochthony measured by ^{13}C addition, and eutrophication by nutrient enrichment (Carpenter and Pace 2018).

Trophic Cascade Experiment

At the start of the trophic cascade experiment, Peter Lake's food web was dominated by planktivorous minnows. In 2008 and 2009, small numbers of adult largemouth bass (*Micropterus salmoides* L.) were gradually added to Peter Lake (Carpenter et al. 2011). A large year class of bass resulted in 2010. Increasingly with bass additions, minnows sought refuge in shallow water and the surrounding bog (Cline et al. 2014a). The decline of minnow numbers in offshore waters was followed by expansion of large-bodied grazing zooplankton (Pace et al. 2013) and decline in chlorophyll concentration (Carpenter et al. 2011). Paul Lake's food web was dominated by largemouth bass throughout the experiment (Carpenter et al. 2011).

Nutrient Enrichment Experiment

Nutrients in the form of inorganic phosphorus and nitrogen were added to enrich Peter Lake in 2013, 2014, and 2015. Nutrients were added daily over the summer season for the first two years and only until early warning signals were obtained in the third year (Pace et al. 2017; Wilkinson et al. 2018). Phytoplankton responded to the additions of nutrients but bloom timing and magnitude varied considerably among years (Wilkinson et al. 2018). Paul Lake, which drains into Peter Lake, did not receive added nutrients and served as an unmanipulated reference ecosystem.

138

High-Frequency Pigment Measurements

140

We used automated pigment measurements during summer stratification to estimate mean exit

times. Data were recorded every 5 minutes.

143

During the Cascade experiment, each lake was monitored with two YSI multi-parameter sondes

(model 6600-V2-4) equipped with optical chlorophyll *a* sensors (model 6025) deployed at a

depth of 0.7 m at a central station (Batt et al. 2013). Chlorophyll *a* is reported in µg/L. We did

not use phycocyanin sensors in this study because cyanobacteria were at low concentrations

throughout and did not reflect the dynamics of the phytoplankton community.

149

During the Enrichment experiment each lake was monitored with a Hydrolab DS5X sonde

including a sensor for phycocyanin fluorescence (model 007291) deployed at a depth of 0.75 m

(Pace et al. 2017). Chlorophyll sensors in this study were not responsive to phytoplankton

blooms unlike direct manual measurements of extracted chlorophyll (SI). Unknown processes

likely related to the presence of large cyanobacterial filaments resulted in low detection of

chlorophyll – a phenomena observed by others (Gregor and Maršálek 2004). Phycocyanin

fluorescence and extracted chlorophyll had similar dynamics consistent with limited microscopic

counts indicating blooms were dominated by cyanobacteria (Wilkinson et al. 2018). Phycocyanin

is reported in relative fluorescence units (RFU). Direct laboratory measurements of phycocyanin

concentration (µg/L) were linearly related to RFU (Pace et al. 2017).

160

Estimation of Mean Exit Time

Mean exit time was estimated by the following steps: (1) Standardize the pigment time series to (Arani et al. 2021b) (S.I. *Dynamic Linear Models*); (2) Test the Markov hypothesis for standardized time series by the Langevin method (S.I. *Assessment of the Markov Property and Stationarity*). (3) Test the stationarity of the standardized time series by the augmented Dickey-Fuller (ADF) test (S.I. *Assessment of the Markov Property and Stationarity*). (4) Using the standardized time series, estimate the deterministic and stochastic components of a Langevin model (system reconstruction); (5) Calculate mean exit time for the ecosystem states of interest.

The in-situ sensors detected chlorophyll for the Cascade experiment and phycocyanin for the Enrichment experiment. We used standardized levels of pigment fluorescence (S.I. *Dynamic Linear Models* and Figures S-1, S-2, S-3, and S-4) as indicators of pigment concentration for both experiments. For the standardized levels reported here, the ADF test rejected the null hypothesis of nonstationarity ($p < 0.01$ for each lake in each experiment) and data exhibited the Markov property (S.I. *Assessment of Markov Property and Stationarity*).

Langevin Analysis

Exit time develops from terms of the Langevin equation [1] as summarized in several works (Rinn et al. 2016; Siegert and Friedrich 2001; Siegert et al. 1998; Tabar 2019). A detailed description of exit time analysis is presented by Arani et al. (2021). We present an abbreviated

183   explanation here. A complete worked example (Peter Lake in the enrichment experiment) is

184   provided as R scripts: https://github.com/SRCarpen/ExitTime_BinMethod_PeterLakeExample

185

186   The time series of standardized levels b_t/s_t were used as state variables (x_t) to estimate the drift-

187   diffusion model known as the Langevin equation

188    $$dx = D_1(x)dt + \sqrt{2D_2(x)}\, dW \qquad\qquad [1]$$

189   (Carpenter and Brock 2011; Rinn et al. 2016; Tabar 2019). The implementation in R is based on

190   Rinn et al. (2016) and the Matlab code of Arani et al. (2021). $D_1(x)$ is the deterministic core of

191   the dynamics called the 'drift' in stochastic dynamic modeling. Its roots $D_1(x) = 0$ are the

192   equilibria. $D_2(x)$, called 'diffusion' in stochastic modeling, is a deterministic function that

193   represents the intensity of the noise as a function of x. The noise source is dW where W stands

194   for the Wiener process, and thus dW represents Gaussian white noise. The fitted drift and

195   diffusion functions are used below in calculations of effective potential, the stationary

196   distribution, and mean exit time.

197

198   In this paper, diffusion functions are plotted using the definition

199

200    $$D_2(x) = \frac{1}{2}\sigma^2(x) \qquad\qquad [2]$$

201

202   Thus $\sigma(x) = \sqrt{2D_2(x)}$, and this conversion allows drift and diffusion to be compared in the

203   same units, pigment standardized level / time.

204

205   *Potential and Effective Potential*

9

206

207   Stability of dynamic systems can be illustrated by potential curves, or "ball and cup" diagrams

208   that show stable points as valleys and unstable points as hilltops. For deterministic systems, the

209   potential curve P(x) is the integral

210

211    $U(x) = \int^{x} D_1(z)dz$ [3]

212

213   where z is a dummy variable and the integral is computed over the relevant range of x.

214

215   The potential U(x) does not account for the noise of the system. Studies of resilience should

216   account for the possibility that random events may change the shape of the potentials

217   (Horsthemke and Lefever 1984). Effects of noise are included in the effective potential, $U_E(x)$

218   (Arani et al. 2021) and we use his function here

219

220    $U_E(x) = -\int^{x} \frac{D_1(z)}{D_2(z)} dz + \log\left(D_2(x)\right)$ [4]

221

222   *Exit Time*

223   For both lakes in both experiments, the drift function D_1 describes a curve with 2 stable

224   equilibria separated by an unstable equilibrium (main text Figs. 1-4). The expected exit times

225   from each stable basin can be estimated by solving the backward Fokker-Planck equation with

226   appropriate boundary conditions for each basin:

227    $D_1(x)\frac{dT}{dx} + D_2(x)\frac{d^2T}{dx^2} = -1$ [5]

228   The solution of this equation, given the boundary conditions, is mean exit time T(x) if the

229   starting state of the system is x. For each basin, we use an absorbing boundary at the middle

230   unstable equilibrium where small random disturbance can cause a shift between basins. For the

231   outer boundaries (left boundary of the left basin, right boundary of the right basin) we use a

232   reflecting boundary to indicate that no shift occurs. If the boundary is absorbing, T(x) = 0 at the

233   boundary, i.e. the exit time is 0 at the unstable edge between basins. If the boundary is reflecting,

234   the derivative $\frac{dT}{dx} = 0$ at the boundary, i.e. there is no change in T(x) at the reflecting boundary.

235   For calculations, we chose the left reflecting boundary slightly above the lower limit of the data

236   and the right reflecting boundary slightly below the upper limit of the data.

237   We solved the boundary-value problem [5] with the bvpSolve() package in R using function

238   bvptwp() (Mazzia et al. 2014). An R script to illustrate the method using a simple ecological

239   model is found at https://github.com/SRCarpen/Exit_Time_R

240

241   Solving for T(x) yields mean exit time as a function of x. It is useful to have a single

242   representative value of exit time for an entire basin. We estimated a basin-wide mean exit time

243   for the full width of each basin as the probability-weighted mean of T(x) with probabilities taken

244   from the normalized stationary density of the Fokker-Planck equation which is computed from

245   D_1 and D_2 (Arani et al. 2021; Horsthemke and Lefever 1984). For example, the mean of T(x) is

246   p(x)T(x) where p(x) is the stationary probability that sums to 1 over all values of x. We

247   integrated the stationary density using the hcubature() function of the cubature() package in R

248   (https://bnaras.github.io/cubature/).

249

250   *Uncertainty of Exit Time*

251

252   To assess uncertainty of exit time, we first bootstrapped the autoregressions by randomizing the

253   errors (ε_t, equation S-1a) with replacement and adding them to the predicted y_t to generate

254   pseudodata (Efron and Tibshirani 1993). The pseudodata series were fit to the DLM (equations

255   S-1) and standardized levels were used to estimate drift and diffusion (equation 2), exit times

256   (equation 5) and the stationary probability distribution. 100 bootstrap cycles were run, and the

257   distribution of exit times was corrected for bias (Efron and Tibshirani 1993).

258

259   *Results*

260

261   **Alternate states and resilience: Cascade experiment**

262

263   Chlorophyll concentration time series during summer stratification for manipulated Peter Lake

264   and reference Paul Lake were measured during the summer stratified seasons of 2008-2011

265   (Figs. S1 and S2).

266

267   Standardized levels of chlorophyll (Fig. 1A) in Peter Lake were used to estimate components of

268   a Langevin model (Fig. 1A). Diffusion (variability) is larger than the deterministic rate of change

269   (drift) (Fig. 1B). We plotted sigma (equation [2]) so that both components have the same units.

270

271   Chlorophyll dynamics in Peter Lake are dominated by noise. Nonetheless the drift function

272   indicates 3 equilibria (3 crossings of the line y=0). The left and right equilibria are stable,

273   because a small increase in chlorophyll decreases the rate of change causing chlorophyll to

274   decrease toward the equilibrium point, and a small decrease in chlorophyll increases the rate of

275   change, restoring chlorophyll toward the equilibrium point. The center equilibrium is unstable

276   because small changes of chlorophyll in either direction cause chlorophyll to shift away from the

277   center equilibrium. Thus the center equilibrium is a threshold separating two alternate stable

278   equilibria. The alternate equilibria represent the minnow dominated (higher chlorophyll) and

279   bass dominated (lower chlorophyll) states. The effective potential (equation 4) shows two

280   distinct stability basins (Fig. 1C).

281

282

283

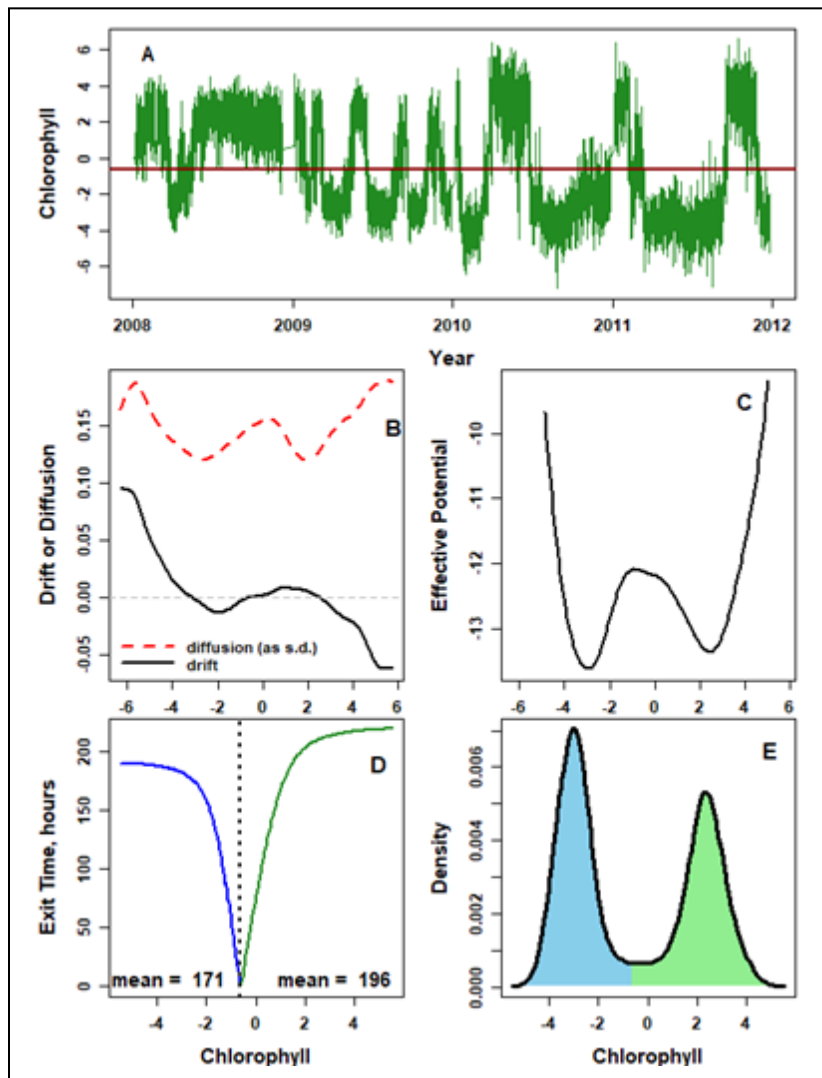284   Figure 1. Resilience analysis of manipulated Peter Lake during the Cascade experiment. (A)

285   Chlorophyll (standardized level) versus year during the experiment. Solid horizontal line denotes

286   the unstable threshold. (B) Drift (black) and diffusion (red) functions versus chlorophyll

287   standardized level. (C) Effective potential versus chlorophyll standardized level. (D) Exit time

288   (hours) versus chlorophyll standardized level, with probability-weighted means, for the two

289   stable basins. Vertical dotted line is the threshold between the basins. (E) Stationary probability

290   density versus chlorophyll standardized level. Shading denotes the low-chlorophyll (blue) and

291   high-chlorophyll (green) basins.

292

14

Figure 2. Resilience analysis of Paul Lake, reference ecosystem for the Cascade experiment. (A) Chlorophyll (standardized level) versus year during the experiment. Solid horizontal line denotes the unstable threshold. (B) Drift (black) and diffusion (red) functions versus chlorophyll standardized level. (C) Effective potential versus chlorophyll standardized level. (D) Exit time (hours) versus chlorophyll standardized level, with probability-weighted means, for the two stable basins. Vertical dotted line is the threshold between the basins. (E) Stationary probability density versus chlorophyll standardized level. Shading denotes the low-chlorophyll (blue) and high-chlorophyll (green) basins.
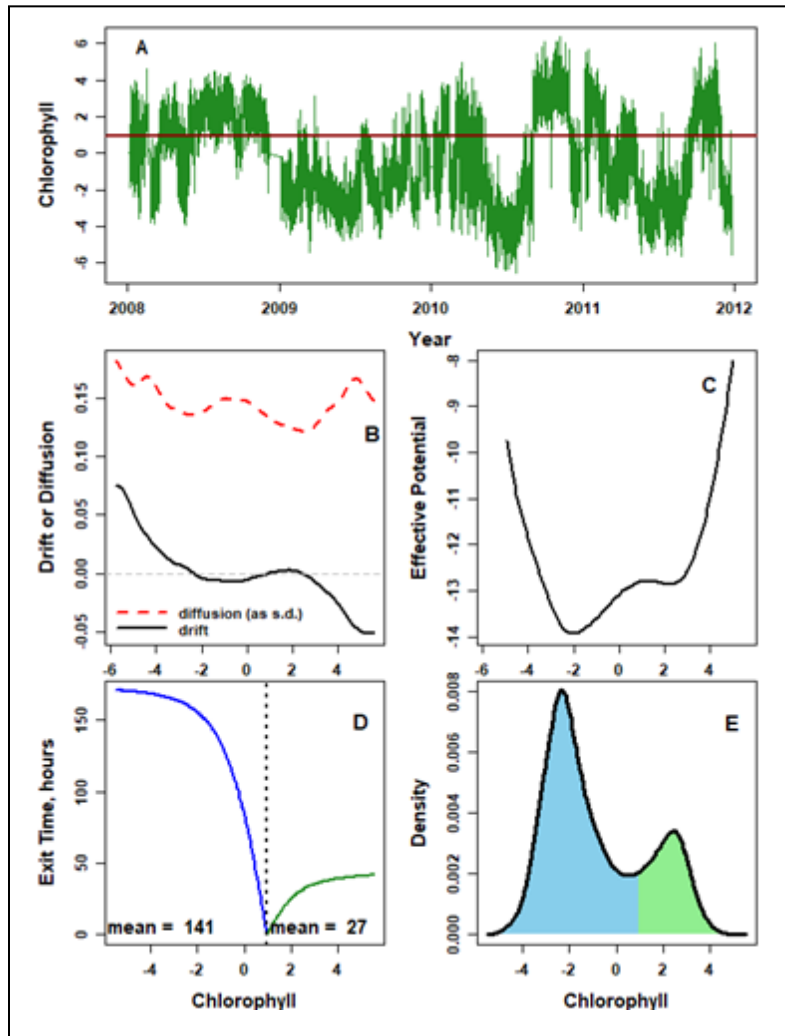
302   Exit time as a function of the initial value of chlorophyll is zero at the unstable equilibrium,

303   because a small perturbation of chlorophyll at that point can shift the ecosystem in either

304   direction (Fig. 1D). Exit times rise as chlorophyll moves either direction from the unstable

305   equilibrium.

306

307   To obtain an average exit time over each basin, we calculate the weighted averages where the

308   weights are the normalized stationary densities for starting values of chlorophyll (Fig. 1D,E).

309   The two states of the ecosystem are apparent in the stationary probability distribution. The mean

310   exit times of the low and high chlorophyll basins are 171 hours and 196 hours, respectively.

311

312   Fluctuations of chlorophyll in Paul Lake represent the baseline variability of an unmanipulated

313   ecosystem (Fig. 2A). Although the diffusion is much larger than the drift, alternate equilibria are

314   discernible (Fig. 2B). Mean exit times of low and high chlorophyll equilibria are 141 and 27

315   hours, respectively (Fig. 2 D,E).

316

317   **Alternate states and resilience: Nutrient Enrichment experiment**

318

319   Phycocyanin RFU were highly variable in manipulated Peter Lake (Fig. 3) and reference Paul

320   Lake during the Enrichment experiment (Fig. 4).

321

322   Standardized levels of phycocyanin in Peter Lake suggest shifts from low to high pigment levels

323   during each year (Fig. 3A). Diffusion (as sigma (equation 2), in the same units as drift) was

324   notably larger than drift (Fig. 3B). The effective potential showed two stable basins, but the

325   high-phycocyanin basin appears shallower than the low-phycocyanin basin (Fig. 3C). Exit times

326   are zero at the unstable transition point between the basins, and rise to the left and right of the

327   transition point (Fig. 3D). The two basins of attraction are evident in the stationary probability

328   density (Fig. 3E). The probability-weighted exit times are 290 hours for the low-phycocyanin

329   basin and 134 hours for the high-phycocyanin basin.

330

331   Paul Lake also exhibited seasonal fluctuations in standardized level of phycocyanin (Fig. 4A).

332   Diffusion was much larger than the drift (Fig. 4B) but nonetheless alternate states are evident in

333   the effective potential (Fig. 4C) and density (Fig. 4E). Exit times are 112 hours for the low-

334   pigment basin and 13 hours for the high-pigment basin (Fig. 4D).
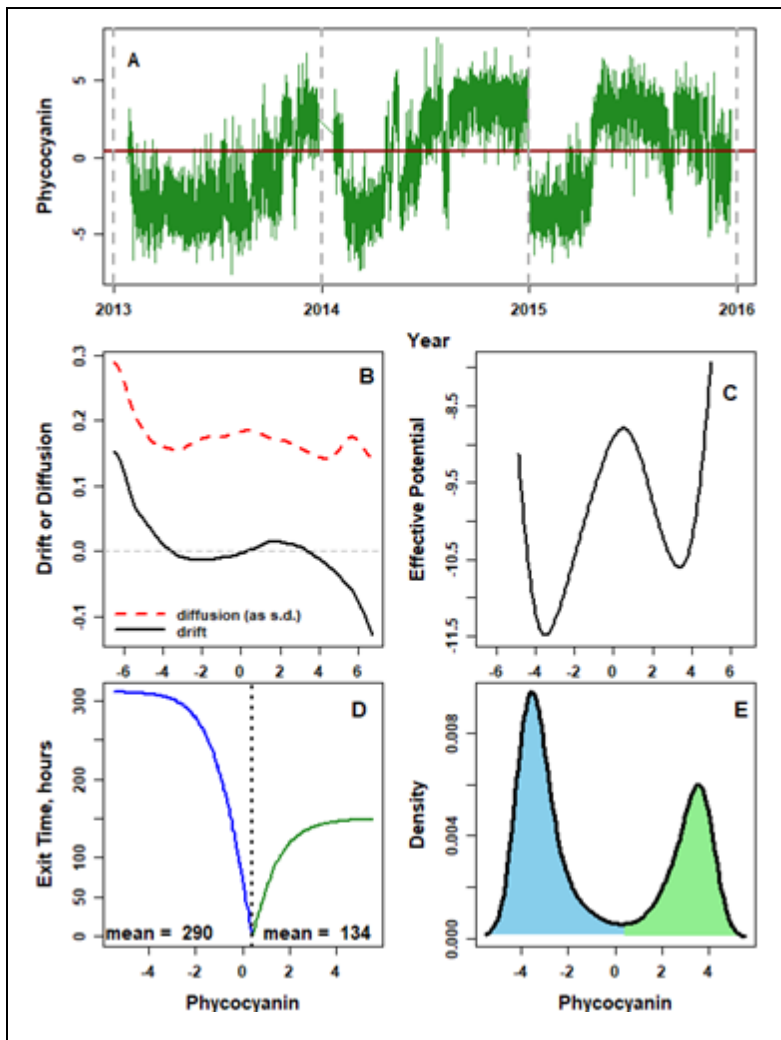
335

336

337   Figure 3. Resilience analysis of enriched Peter Lake during the Enrichment experiment. (A)

338   Phycocyanin (standardized level) versus year during the experiment. Solid horizontal line

339   denotes the unstable equilibrium. (B) Drift (black) and diffusion (red) functions versus

340   phycocyanin standardized level. (C) Effective potential versus phycocyanin standardized level.

341   (D) Exit time (hours) versus phycocyanin standardized level, with probability-weighted means,

342   for the two stable basins. Vertical dotted line is the threshold between the basins. (E) Stationary

343   probability density versus phycocyanin standardized level. Shading denotes the low-phycocyanin

344   (blue) and high-phycocyanin (green) basins.

345

346

Figure 4. Resilience analysis of Paul Lake during the Enrichment experiment. (A) Phycocyanin

(standardized level) versus year during the experiment. Solid line denotes the unstable

equilibrium. (B) Drift (black) and diffusion (red) functions versus phycocyanin standardized

level. (C) Effective potential versus phycocyanin standardized level. (D) Exit time (hours) versus

phycocyanin standardized level, with probability-weighted means, for the two stable basins.

Vertical dotted line is the threshold between the basins. (E) Stationary probability density versus

phycocyanin standardized level. Shading denotes the low-phycocyanin (blue) and high-

phycocyanin (green) basins.
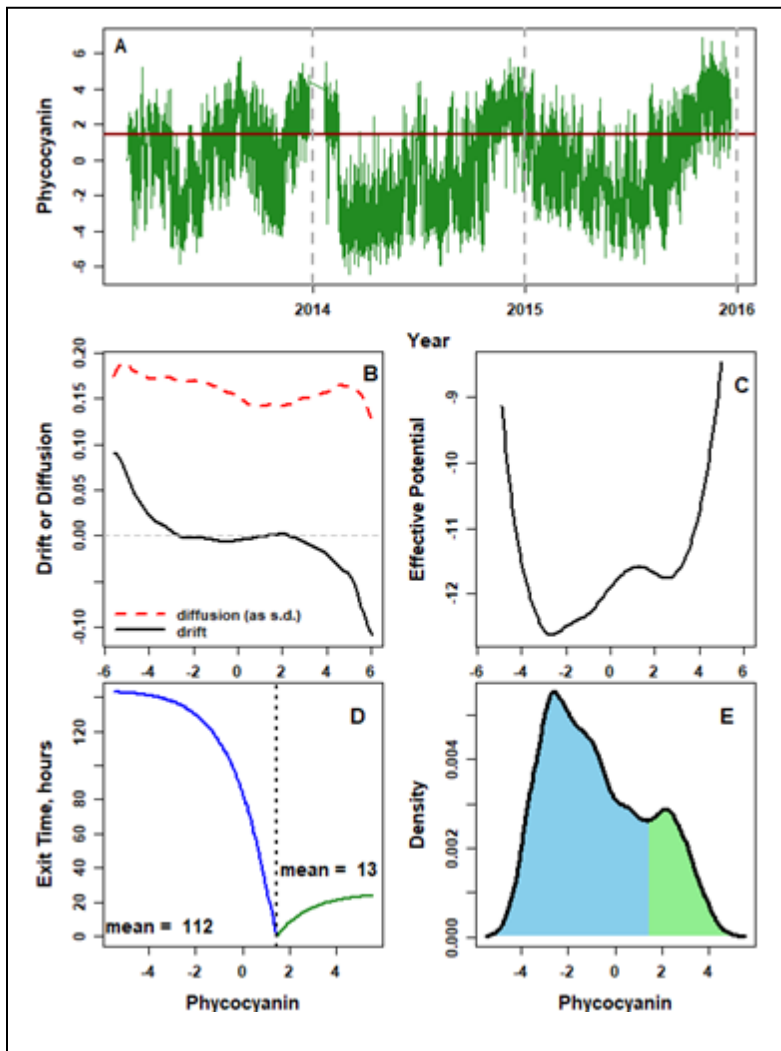
Validation of the Models

For each dataset the one-step predictions of the fitted Langevin equations compared to data had a lower negative log likelihood than a hypothetical model with constant drift (S.I. *Model Validation*). To visualize the goodness of fit we compared one-step conditional probabilities predicted by the Langevin equations with the observed one-step changes of the data for selected initial points quantiles in each lake in each experiment (S.I. *Model Validation* and Fig. S5). Predicted distributions closely matched observed distributions.

Uncertainty of Exit Time Estimates

Distributions of the deterministic equilibria (zeroes of the drift function) were estimated by bootstrapping (S.I. Figs. S6 and S7). For Peter Lake, each bootstrapped pseudo-dataset, 100 for each experiment, had three equilibria, two stable equilibria separated by an unstable threshold. The variability of estimated equilibria is relatively narrow and equilibria are well-separated on the pigment axes (Fig. S6). For Paul Lake equilibria were distinct and variability was modest (Fig. S7).

Distributions of mean exit time from 100 bootstrap cycles were computed for both stable basins in both experiments (S.I. Figs. S8 and S9). Exit time includes the stochasticity of the dynamics (diffusion). Patterns of the distributions were different among experiments, lakes, and stability basins.

380   In manipulated Peter Lake, exit times were longer than in unmanipulated Paul Lake based on

381   interquartile ranges (Fig. 5). Exit time from the low-pigment basin was longer than exit time

382   from the high-pigment basin in Paul Lake. In Peter Lake for the Cascade experiment the high-

383   pigment equilibrium had longer exit time than the low-pigment equilibrium. In the Enrichment

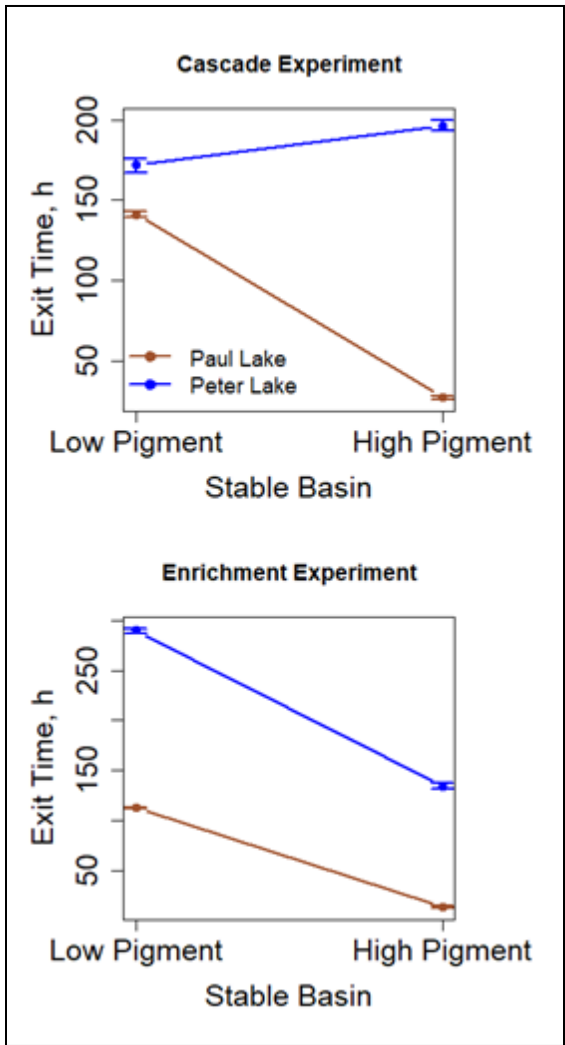384   experiment this pattern was reversed with shorter exit time in the high-pigment equilibrium.

385

Figure 5. Exit time for low- and high-pigment stable basins for both lakes during the Cascade and Enrichment experiments. Error bars show the interquartile range (25th to 75th percentile) and circle shows the median (50th percentile) of 100 bootstrap samples (S.I.).

398

399   *Discussion*

400   The long-term condition of both lakes is the low-pigment state. In Peter Lake the manipulations

401   caused short-term excursions into the high-pigment state, but by different mechanisms. In the

402   Cascade experiment, intervals of high chlorophyll were caused by fluctuations in grazing

403   associated with movement of planktivorous fishes between littoral and pelagic habitats (Cline et

404   al. 2014b; Pace et al. 2013). In the Nutrient Enrichment experiment, intervals of high

405   phycocyanin were associated with accumulation of phosphorus and nitrogen in phytoplankton

406   (Wilkinson et al. 2018). When manipulations ended, the ecosystem returned to the low-pigment

407   pre-manipulation state. For both experiments, phase-randomized surrogate time series did not

408   have alternate states, suggesting that alternate states were not likely to be detected by chance

409   (S.I. *Could Alternate States be Detected by Chance?*).

410

411   In Paul Lake, fluctuations of pigment concentrations are due to the routine dynamics of

412   phytoplankton in a variable physical-chemical environment, interacting with grazers in an

413   ecosystem that was not manipulated. Note that Paul Lake lies upstream of Peter Lake, was

414   sampled using a separate boat, and was not contaminated with added nutrients. Chlorophyll

415   fluctuations in Paul Lake show occasional brief peaks in the epilimnion (Fig. S2) as seen in

416   previous studies (Carpenter et al. 2001; Carpenter and Kitchell 1993). Weekly phytoplankton

417   counts in Paul Lake from 1984-1997 showed both absence and occasional peaks of

418   Cyanobacteria that are consistent with the patterns we observed in high-frequency phycocyanin

419   data (Cottingham et al. 1998). These fluctuations could have appeared as alternate states in our

420   analysis.

421

422   We were surprised to see alternate states in the high-frequency pigment data from Paul Lake.

423   The experiments were designed initially to test dynamic indicators of resilience. In Peter Lake,

424   several dynamic indicators provided early warnings of loss of resilience but no indications of

425   declining resilience were detected in Paul Lake (Batt et al. 2013; Carpenter et al. 2011; Cline et

426   al. 2014a; Pace et al. 2017; Pace et al. 2013; Wilkinson et al. 2018).

427

428   We considered the possibility that cyclic fluctuations in irradiance, temperature or other

429   variables could appear to be alternate states in sensor data. During each experiment in each lake,

430   daily samples were taken, returned to the laboratory, and analyzed by fluorometry to measure

431   chlorophyll *a* concentration (Carpenter et al. 2011; Pace et al. 2017). Drift functions of the

432   Langevin equation [1] for daily chlorophyll time series show alternate states for the manipulated

433   lake, Peter Lake, but not for the reference Paul Lake (Fig. S-10 and S.I. *Alternate States in Daily*

434   *Chlorophyll Time Series*). However, the diffusion component is relatively large, consistent with

435   the sensor data. Because of the daily time step and small sample size (about 120 daily samples

436   per year versus 288 sensor samples per day, or about 34,560 sensor samples per year in each

437   lake), we did not attempt to estimate exit time from the daily data. Patterns in the daily data are

438   consistent with the alternate states we detected in Peter Lake but ambiguous with regard to the

439   alternate states we detected in Paul Lake. Further research using high-frequency pigment

440   measurements in a wider variety of aquatic environments is needed to improve understanding of

441   alternate states of phytoplankton and the response of stochastic indicators such as exit time.

442

443   An exit event occurs when the pigment line crosses the unstable equilibrium that separates the

444   two basins (Figures 1A, 2A, 3A, 4A). Most of the intervals between exit events are short, and

445   some quick events are hidden by the width of the plotted lines. Thus the mean exit times range

446   from about 1 to 10 days due to the dominance of short events (Fig. 5). These rather short mean

447   exit times are another indication of the high variability of the time series.

448

449   To be useful an indicator of stochastic resilience should be repeatable, comparable among

450   ecosystems, responsive to changes in resilience, and have low-to-moderate uncertainty for real-

451   world time series. In addition, for our method the time series to be analyzed should meet the

452   assumptions of the Langevin method. For these sensors and these lakes the standardized levels

453   analyzed here meet these conditions. Different data standardizations may be appropriate for

454   different ecosystems or sensors.

455

456   In summary, resilience of phytoplankton biomass (as measured here by their pigments) in lake

457   ecosystems may depend on slowly-changing variables such as watershed sources of nutrients and

458   colored DOC, sediment release of nutrients, grazer dynamics, and apex predators. Gradual trends

459   of such variables reduce resilience and increase the likelihood that random events can cause a

460   regime shift (Holling 1973a; Holling 1973b; Scheffer et al. 2001). Our experiments simulated

461   gradual forcing of Peter Lake by trophic cascades or nutrients. Pigment concentration, especially

462   in sensor optical measurements, is highly variable and this variance strongly affects resilience

463   measured using exit time and likely other stochastic indicators. The temporal fluctuations of

464   chlorophyll are large enough that thresholds are crossed every few days when measured by high-

465   frequency sensors during multi-year whole-lake experiments. We suspect that a decades-long

466   perspective of high-frequency measurements could reveal much longer exit times for past states

467   of Peter Lake, consistent with patterns seen in paleolimnological records (Leavitt et al. 1989).

468   Nonetheless we have shown a pathway for comparative resilience studies of lake ecosystems

469   using resilience measures that are consistent with Holling's (Holling 1973a) emphasis of random

470   fluctuations as a key element of resilience. The challenge is to build long-term highly-resolved

471   datasets needed to measure stochastic variates that may provide a quantitative indicators for

472   comparing resilience among aquatic ecosystems.

473

474   <u>Acknowledgements</u>

475

487

Literature Cited

Arani, B. M. S., S. R. Carpenter, L. Lahti, E. H. van Nes, and M. Scheffer. 2021. Exit time as a measure of ecological resilience. Science **372:** eaay4895.

Batt, R. D., S. R. Carpenter, J. J. Cole, M. L. Pace, and R. A. Johnson. 2013. Changes in ecosystem resilience detected in automated measures of ecosystem metabolism during a whole-lake manipulation. Proceedings of the National Academy of Sciences **110:** 17398-17403.

Carpenter, S. R. 2003. Regime Shifts in Lake Ecosystems: Pattern and Variation. Ecology Institute.

Carpenter, S. R., and W. A. Brock. 2011. Early warnings of unknown nonlinear shifts: a nonparametric approach. Ecology **92:** 2196-2201.

Carpenter, S. R. and others 2001. Trophic cascades, nutrients and lake productivity: Whole-lake experiments. Ecological Monographs **71:** 163-186.

Carpenter, S. R. and others 2011. Early Warnings of Regime Shifts: A Whole-Ecosystem Experiment. Science **332:** 1079-1082.

Carpenter, S. R., and J. F. Kitchell [eds.]. 1993. Trophic Cascades in Lakes. Cambridge University Press.

Carpenter, S. R., and M. L. Pace. 2018. Synthesis of a 33-yr series of whole-lake experiments: Effects of nutrients, grazers, and precipitation-driven water color on chlorophyll. Limnology and Oceanography Letters **3:** 419-427.

Carpenter, S. R., and G. D. Peterson. 2019. C. S. 'Buzz' Holling, 6 December 1930 – 16 August 2019. Nature Sustainability **2:** 997-998.

Cline, T. J. and others 2014a. Early warnings of regime shifts: evaluation of spatial indicators from a whole-ecosystem experiment. Ecosphere **5:** 1-13.

---. 2014b. Early warnings of regime shifts: evaluation of spatial indicators from a whole-ecosystem experiment. Ecosphere **5:** art102.

512   Cottingham, K. L., S. R. Carpenter, and A. L. S. Amand. 1998. Responses of epilimnetic phytoplankton to

513   experimental nutrient enrichment in three small seepage lakes. Journal of Plankton Research **20:**

514   1889-1914.

515   Efron, B., and R. J. Tibshirani. 1993. An Introduction to the Bootstrap. Chapman and Hall.

516   Elser, M. M., J. J. Elser, and S. R. Carpenter. 1986. Paul and Peter Lakes: A Liming Experiment Revisited.

517   The American Midland Naturalist **116:** 282-295.

518   Gregor, J., and B. Maršálek. 2004. Freshwater phytoplankton quantification by chlorophyll a: a

519   comparative study of in vitro, in vivo and in situ methods. Water Research **38:** 517-522.

520   Holling, C. S. 1973. Resilience and stability of ecological systems. Annual Review of Ecology and

521   Systematics **4:** 1-23.

522   Horsthemke, W., and R. Lefever. 1984. Noise-Induced Transitions: Theory and Applications in Physics,

523   Chemistry and Biology. Springer-Verlag.

524   Kleinen, T., H. Held, and G. Petschel-Held. 2003. The potential role of spectral properties in detecting

525   thresholds in the Earth system: application to the thermohaline circulation. Ocean Dynamics **53:**

526   53-63.

527   Leavitt, P. R., S. R. Carpenter, and J. F. Kitchell. 1989. Whole-lake experiments: The annual record of

528   fossil pigments and zooplankton. Limnology and Oceanography **34:** 700-717.

529   Mazzia, F., J. Cash, and K. Soetart. 2014. Solving boundary value problems in the open source software

530   R: Package bvpSolve. Opuscula Mathematica **34:** 387-403.

531   Pace, M. L. and others 2017. Reversal of a cyanobacterial bloom in response to early warnings.

532   Proceedings of the National Academy of Sciences **114:** 352-357.

533   Pace, M. L., S. R. Carpenter, R. A. Johnson, and J. T. Kurzweil. 2013. Zooplankton provide early warnings

534   of a regime shift in a whole-lake manipulation. Limnology and Oceanography **58:** 525-532.

535   Pole, A., M. West, and J. Harrison. 1994. Applied Bayesian forecasting and time series analysis. Chapman

536   & Hall.

537   Rinn, P., P. G. Lind, M. Wachter, and J. Peinke. 2016. The Langevin approach: an R package for modeling

538   Markov processes. Journal of Open Research Software **4:** e34.

539   Scheffer, M. 1998. Ecology of Shallow Lakes. Springer-Verlag.

540   ---. 2009. Critical transitions in nature and society. Princeton University Press.

541   Scheffer, M., S. Carpenter, J. A. Foley, C. Folke, and B. Walker. 2001. Catastrophic shifts in ecosystems.

542   Nature **413:** 591-596.

543   Scheffer, M., S. R. Carpenter, V. Dakos, and E. H. v. Nes. 2015. Generic Indicators of Ecological Resilience:

544   Inferring the Chance of a Critical Transition. Annual Review of Ecology, Evolution, and

545   Systematics **46:** 145-167.

546   Siegert, S., and R. Friedrich. 2001. Modeling of nonlinear Lévy processes by data analysis. Physical

547   review. E, Statistical, nonlinear, and soft matter physics **64:** 041107.

548   Siegert, S., R. Friedrich, and J. Peinke. 1998. Analysis of data sets of stochastic systems. Physics Letters A

549   **243:** 275-280.

550   Tabar, M. R. R. 2019. Analysis and Data-Based Reconstruction of Complex Nonlinear Dynamical Systems.

551   Springer Nature.

552   West, M., and P. J. Harrison. 1989. Bayesian Forecasting and Dynamic Models. Springer-Verlag.

553   Wilkinson, G. M. and others 2018. Early warning signals precede cyanobacterial blooms in multiple

554   whole-lake experiments. Ecological Monographs **88:** 188-203.

555

SUPPORTING INFORMATION

for

Resilience of Chlorophyll Dynamics to Trophic Cascades and Nutrient Enrichment

Stephen R. Carpenter*[1], Babak M.S. Arani[2], Egbert H. Van Nes[2], Marten Scheffer[2],
Michael L. Pace[3]

[1] Center for Limnology, University of Wisconsin, Madison, WI 53706 U.S.A.

[2] Aquatic Ecology and Water Quality Management, Wageningen University, P.O. Box 47, 6700 AA Wageningen, The Netherlands

[3] Department of Environmental Sciences, University of Virginia, Charlottesville, Virginia 22904 U.S.A.

*Correspondence: Steve.Carpenter@wisc.edu

Contents

40   ***Dynamic Linear Models***

41

42   Dynamic linear models are forecasting models updated sequentially from observations by Bayes'
43   formula (West and Harrison 1989). We applied dynamic linear models or DLMs to high-
44   frequency time series from each experiment to standardize the data prior to Langevin analysis.
45   The time varying-models separate the pigment fluctuations into components corresponding to
46   time-varying level, autocorrelated change, errors of each model component, and observation
47   error (Carpenter et al. 2020; Pole et al. 1994; West and Harrison 1989).

48

49   In the DLM for a time-varying autoregression, the intercept b_t and autocorrelation coefficients ϕ_t
50   vary over time, according to independent random walks. For a lag-1 autoregressive process, the
51   data or observation equation is

52     $y_{t+1} = b_t + \phi_t y_t + \varepsilon_t$ [S-1a]

53   where y is the observed time series of pigment concentrations, b_t is the time series of the
54   intercept or level parameter, ϕ_t is the time series of the autoregressive parameter, and ε_t is the
55   time series of observation errors. The evolution of parameters over time follows the system
56   equations, one for each parameter

57     $b_t = b_{t-1} + \omega_{b,t-1}$ [S-1b]

58     $\phi_t = \phi_{t-1} + \omega_{\phi,t-1}$ [S-1c]

59   Where $\omega_{b,t-1}$ is the time series of process errors in the level b_t, and $\omega_{\phi,t-1}$ is the time series of
60   process errors in the autoregression coefficient ϕ. The observation errors and the two process
61   errors are Normal processes independent of each other and over time. By choosing prior
62   distributions for initial values, the full model was estimated sequentially from the data by
63   Bayesian updating (West and Harrison 1989).

64   Time series of b_t, ϕ_t, their time-varying standard errors s_{bt} and $s_{\phi,t}$, one-step predictions $\tilde{y}_t$ and
65   the observation standard error $s_{\varepsilon,t}$ result from fits of [S1] to the time series x_t. We used the
66   AR(1) model because it had lower AIC than AR(2) or AR(3) models. Equations [S-1] were
67   estimated using the Bayesian updating algorithm in Table 3.2 of Pole et al. (1994). A sample R
68   script is included as Step1 of the worked example posted on
69   https://github.com/SRCarpen/ExitTime_BinMethod_PeterLakeExample

70   The time series b_t tracks changes in the level of the data and its standard error is $s_{b,t}$ the time-
71   varying error of the level. The standardized intercept $b_t/s_{b,t}$ combines the time-varying level of
72   pigment concentration scaled by its time-varying noise. We used time series of the standardized
73   intercept, or level, $b_t/s_{b,t}$ as the index of time-varying pigment concentration for subsequent
74   analyses. Simulations show that the standardized level correctly identifies alternate states when
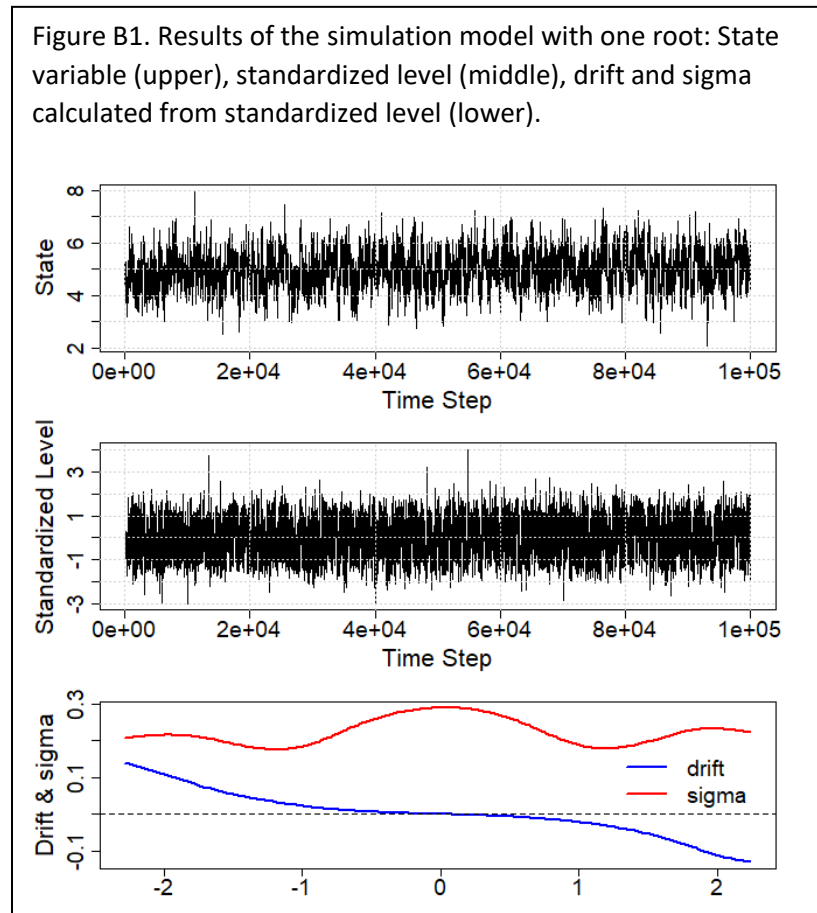75   they are present, and does not suggest alternate states if they are absent (Box S1).

76

77

78 **Box S1**. Simulation results for a model with one stable equilibrium and a model with alternate
79 states. Each figure shows a simulated time series of 100,000 steps, the standardized level from a
80 DLM fit to the data, and drift and diffusion curves estimated from the standardized level.

81 The 1-root model represents dynamics of a conservative solute, such as chloride, in a lake.
82 Dynamics follow

83 dx = (a – bx)dt + c dW   [B-1]

84 where input a = 5, loss coefficient b = 1, and the standard deviation of environmental noise c =
85 1. There is a single stable equilibrium at a/b. The model was solved by the Euler-Maruyama
86 method. The resulting time series and the standardized level have one equilibrium (Fig. B-1).

87

Figure B1. Results of the simulation model with one root: State variable (upper), standardized level (middle), drift and sigma calculated from standardized level (lower).
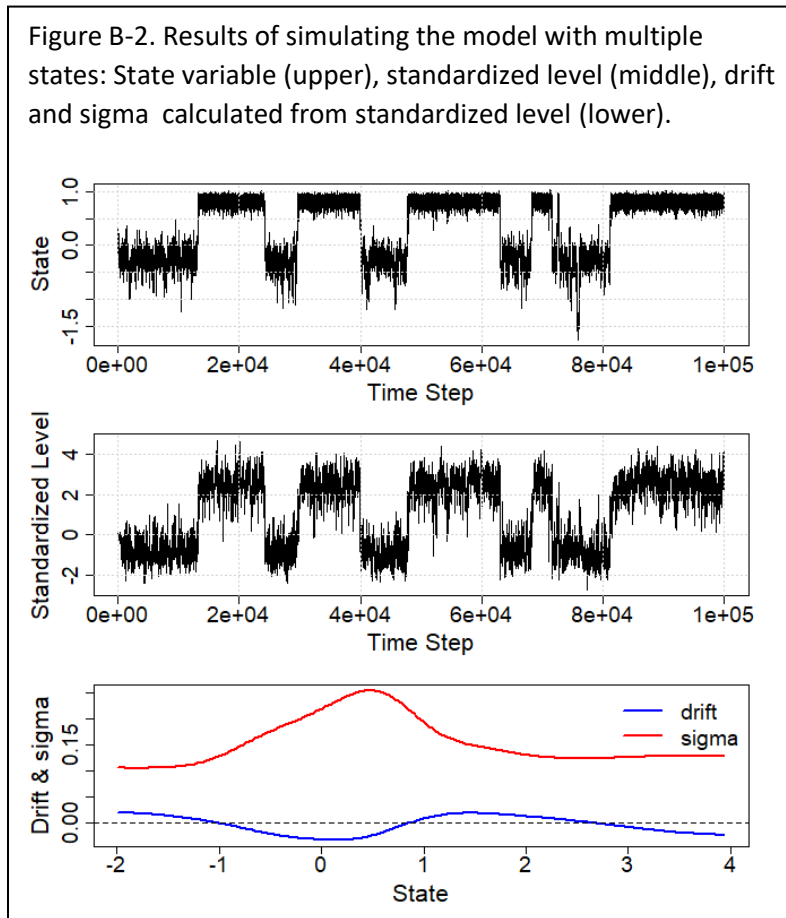
104

105

106

107

108

109 The model from May (1977) of an exploited population was discretized following Ives and
110 Dakos (Ives and Dakos 2012) as

111 $\quad$ x1 = x0 exp(f(x0) + Z0 – s^2/2) $\qquad\qquad\qquad$ [B2]

112 $\quad$ f(x) = rx(1 – (x/K)) – ax^q/(x^q + h^q)) $\qquad\qquad$ [B3]

113 with intrinsic growth rate r = 1, carrying capacity K = 10, curvature of the functional response q
114 = 2, maximum loss rate a = 2.2, predation half-saturation h = 1, normally-distributed
115 environmental noise Z0, and standard deviation of the noise s = 0.4. The resulting time series
116 has 3 equilibria, as does the standardized level time series (Figure B2).

117

118
119
120

Figure B-2. Results of simulating the model with multiple states: State variable (upper), standardized level (middle), drift and sigma calculated from standardized level (lower).

134 **END BOX S1** ---

140   Results of dynamic linear models for the manipulated ecosystem, Peter Lake, and reference
141   ecosystem, Paul Lake, in both the Cascade and Enrichment experiments are presented in Figures
142   S1 – S4. Chlorophyll in Peter Lake shows great variability from point to point but nonetheless
143   broad fluctuations are discernible (Fig.S-1A). The time series of the level, b_t, reflects the broad
144   patterns of chlorophyll but also some outliers (Fig. S-1B). The time series of standard error of the
145   level, $s_{b,t}$ shows that some of the outliers have high error (Fig. S-1C). The standardized level, or
146   ratio of level to its standard error $b_t/s_{b,t}$ retains the broad pattern of the chlorophyll time series
147   (Fig. S-1D). Point-to-point variability is large, as seen in the chlorophyll data, and appears
148   consistent throughout the time series.

149

150   The same sequence of steps is presented for Paul Lake in the Cascade experiment (Fig. S-2) and
151   both lakes in the Enrichment experiment, Peter (Fig. S-3) and Paul (Fig. S-4). Standardized
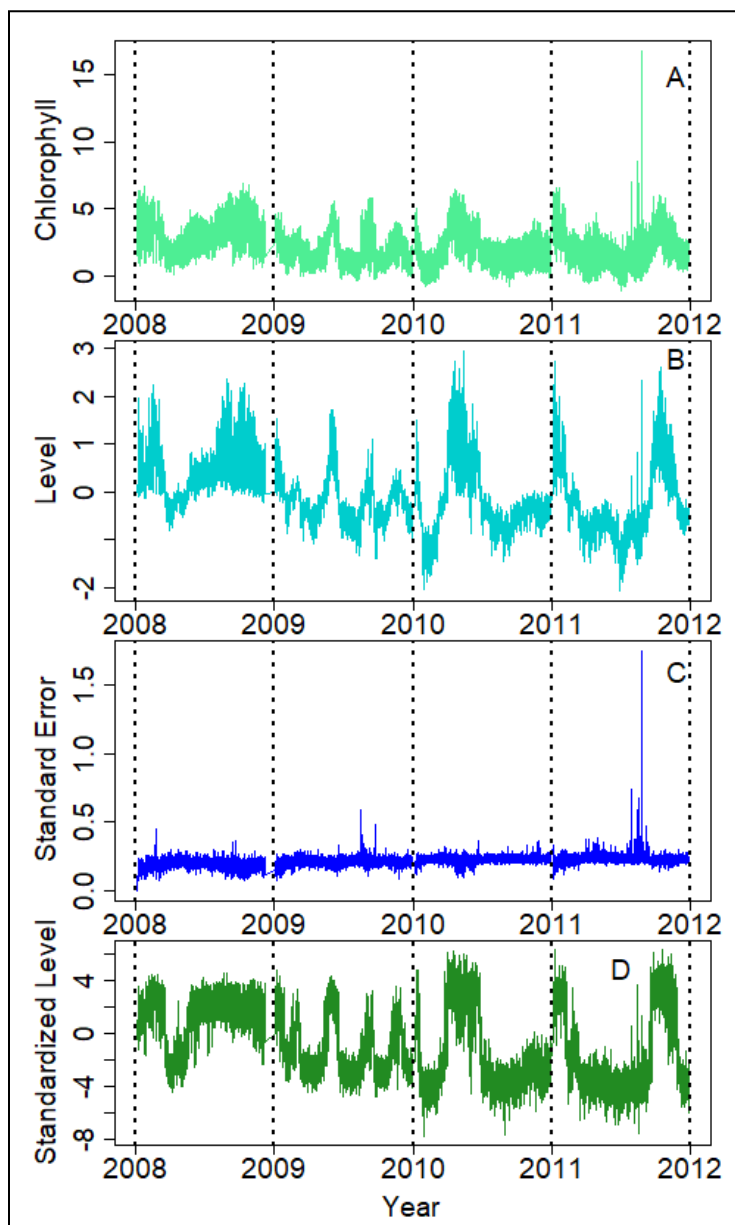152   levels were used for subsequent estimates of exit time.

Figure S-1. Cascade experiment: (A) chlorophyll a (μg L^{-1}) measured every 5 minutes in Peter Lake during the summer stratification periods of 2008-2011; (B) Level b_t (intercept of time-varying autoregression) (μg L^{-1}); (C) standard error of level $s_{b,t}$ (μg L^{-1}); (D) standardized level ($b_t / s_{b,t}$), dimensionless.
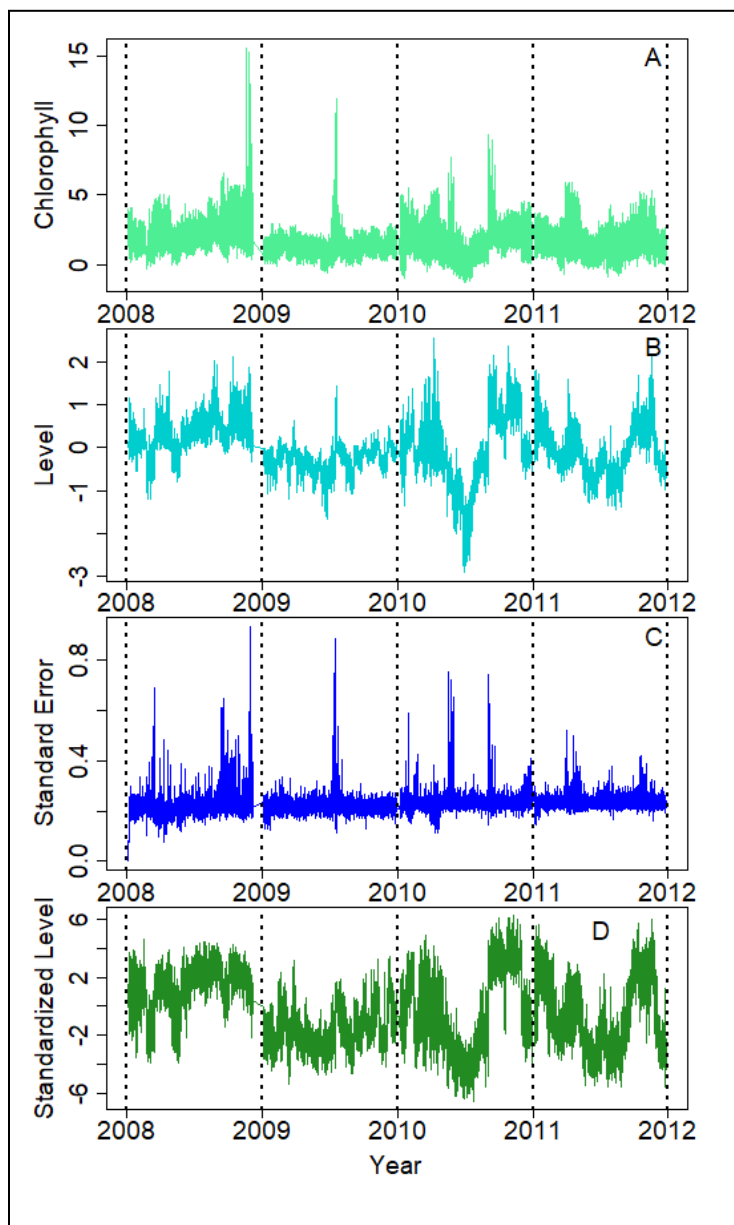
170 Figure S-2. Paul Lake, reference ecosystem for the cascade experiment:
171 (A) chlorophyll a (μg L^{-1}) measured every 5 minutes during the summer stratification periods of
172 2008-2011; (B) Level b_t (intercept of time-varying autoregression) (μg L^{-1}); (C) standard error of
173 level $s_{b,t}$ (μg L^{-1}); (D) standardized level (b_t / $s_{b,t}$, dimensionless).

174

175

176 Figure S-3. Enrichment experiment results in Peter Lake: (A) phycocyanin (RFU) measured
177 every 5 minutes in Peter Lake during the summer stratification periods of 2013-2015; (B) Level
178 b_t (intercept of time-varying autoregression) (RFU); (C) standard error of level $s_{b,t}$ (RFU); (D)
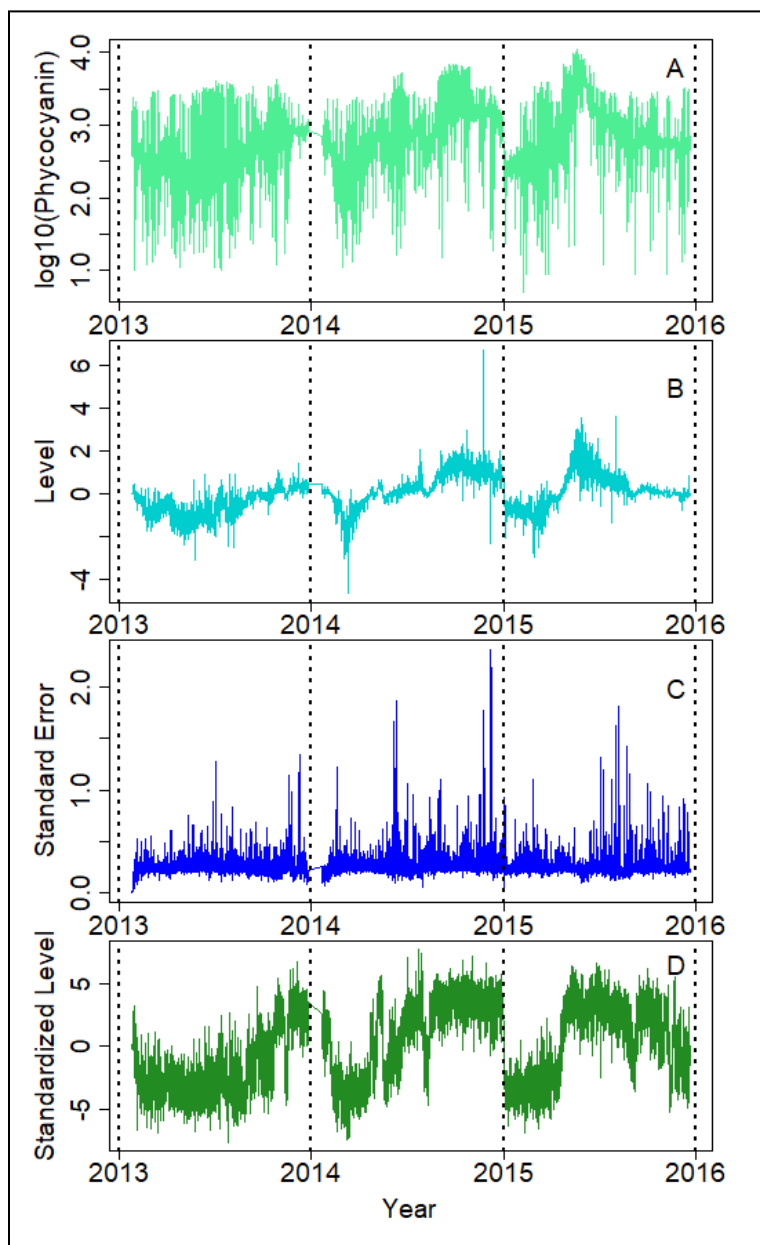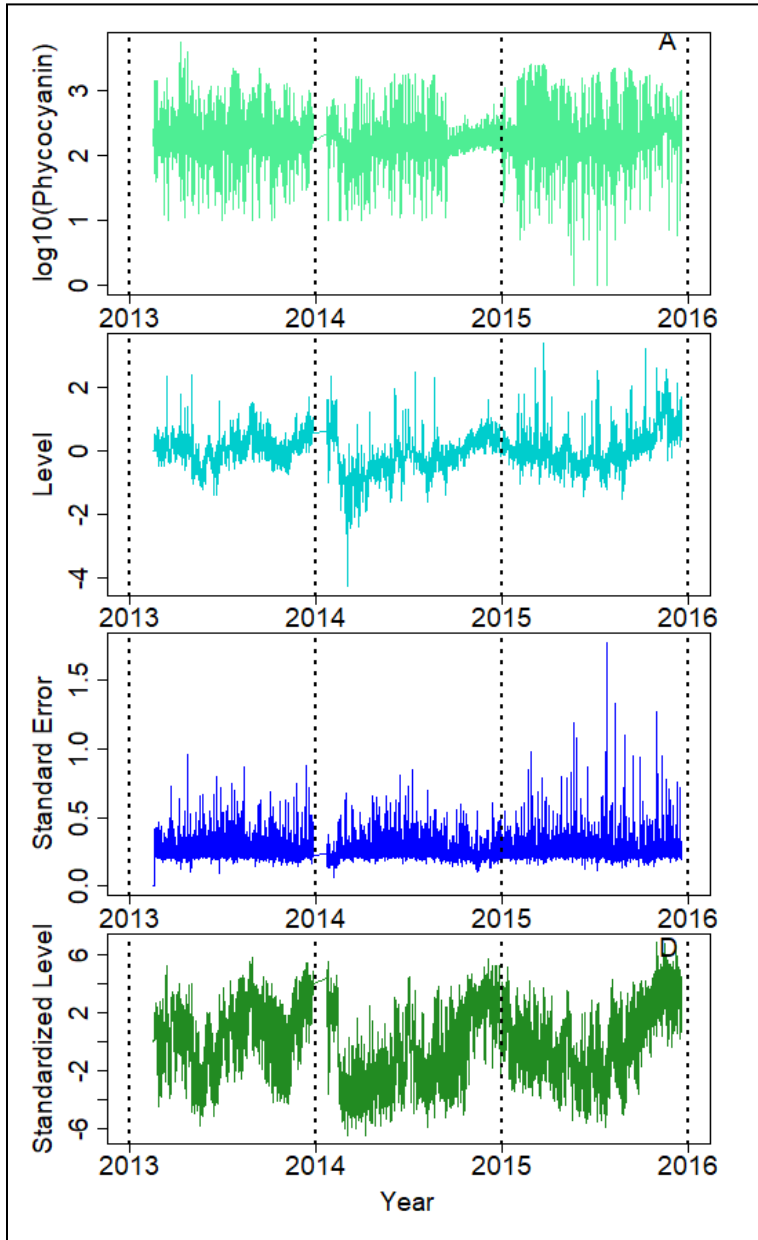179 standardized level ($b_t / s_{b,t}$, dimensionless).

Figure S-4. Paul Lake, reference lake for the enrichment experiment: (A) phycocyanin (RFU) measured every 5 minutes during the summer stratification periods of 2013-2015; (B) Level b_t (intercept of time-varying autoregression) (RFU); (C) standard error of level $s_{b.t}$ (RFU); (D) standardized level ($b_t / s_{b,t}$, dimensionless).

### *Assessment of the Markov Property and Stationarity*

The Langevin approach requires time series with frequent observations and long enough duration to include state transitions (Arani et al. 2021). The dynamics should be represented by the first two moments (i.e. D4 < D2) (Arani et al. 2021; Friedrich et al. 2011). The standardized levels analyzed in this paper met these assumptions.

We assessed stationarity of the data using the augmented Dickey-Fuller (ADF) test (adf.test() in the tseries() library of R) (https://cran.r-project.org/web/packages/tseries/). The null hypothesis of the ADF is that the data are non-stationary. For both lakes in both experiments this hypothesis was rejected (p < 0.01). We infer that the data are approximately stationary as expected for Langevin analysis.

In addition the input data for the Langevin analysis should have the Markov property, i.e. each observation depends only on the previous observation and be stationary, i.e. the statistical properties are approximately constant over time (Arani et al. 2021). We tested the Markov hypothesis for each time series of standard level using the Box-Ljung and Rank tests in the R library spgs() available at https://rdrr.io/cran/spgs/man/spgs-package.html. In all cases the Markov property could not be rejected (p > 0.01).

As a further test of the Markov property we calculated the so-called 'Markov-Einstein time (ME) scale' using the Chapman-Kolmogorov equation (Arani et al. 2021; Tabar 2019). The ME time scale is determined as a time lag where a χ^2 distance (equation 16.12 of Tabar 2019) is minimal between $p(x_3, t_3 | x_1, t_1)$ calculated directly from data versus from the Chapman-Kolmogorov equation. Note that data are Markov if the ME time scale equals one. For our time series the ME time scale is 3 to 6 steps (Figure S5). Although our data are near-Markov we still follow the Langevin approach since it is safer to do so rather than trying to follow more advanced reconstruction schemes designed to account for systems driven by colored noise (Hassanibesheli et al. 2020).

274 Figure S5. Chi-square distance between the data and the Chapman-Kolmogorov equation versus
275 time lag for Peter Lake in the (A) Cascade and (B) Enrichment experiments, and for Paul Lake in
276 the (C) Cascade and (D) Enrichment experiments

277

295
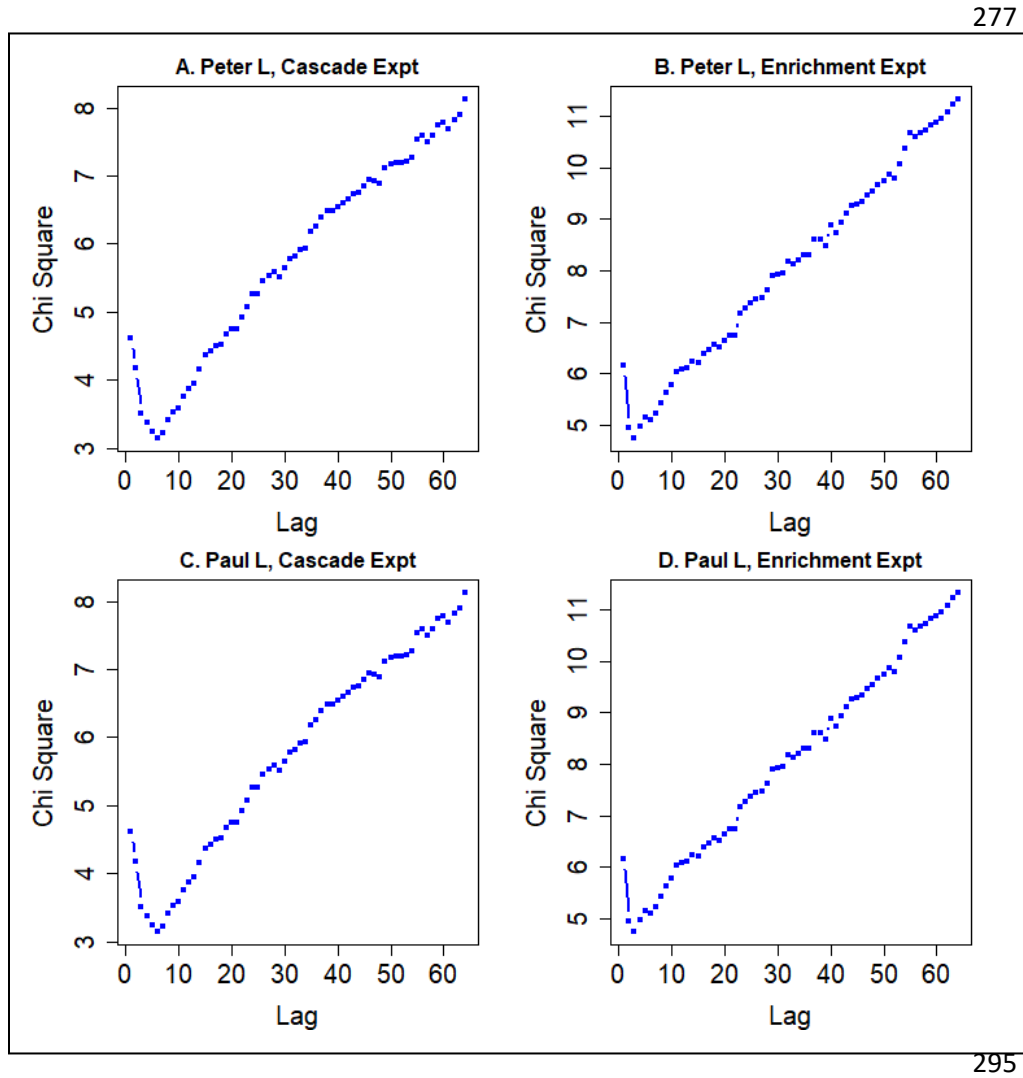
296 As further illustration that our data conform to the Markov property we compared the data to
297 Chapman-Kolmogorov equation (Fig. S6). A stochastic process x_k sampled at times t_k is said to
298 be Markovian if

299 $$p(x_k, t_k | x_{k-1}, t_{k-1}, \ldots, x_1, t_1) = p(x_k, t_k | x_{k-1}, t_{k-1}) \qquad [S2]$$

300 This equation means that the process at any time depends on its previous state only and has no
301 dependency to the remaining past states. There are several ways to assess the Markov property
302 (Tabar 2019). We compared the data to the Chapman-Kolmogorov (CK) equation

303 $$p(x_3, t_3 | x_1, t_1) = \int p(x_3, t_3 | x_2, t_2) \, p(x_2, t_2 | x_1, t_1) \, dx_2 \qquad [S3]$$

304 which is valid for all Markov processes. The conditional probability $p(x_3, t_3 | x_1, t_1)$ is calculated
305 in two ways: directly by the data and by the right side of CK equation via two smaller steps at all

306   intermediate times t_2 ($t_1 < t_2 < t_3$) (Figure S5). This process is suitable because the
307   standardized level time series are approximately stationary (Tabar 2019). The data closely adhere
308   to the Chapman-Kolmogorov equation indicating consistency with the Markov property.

309   Figure S6. Validation of the Chapman Kolmogorov (CK) equation for a time lag of 1, i.e., the
310   time scale of data, where a close match is observed between $P(x_3|x_1)$ being calculated directly
311   by data (black) and by the right side of eq S3, showing that all datasets are a good approximation
312   of the Markov property. In $P(x_3|x_1)$, x_1 is the initial state which is treated a bin-wise manner so
313   that each peak in the figures represent a particular value of x_1.
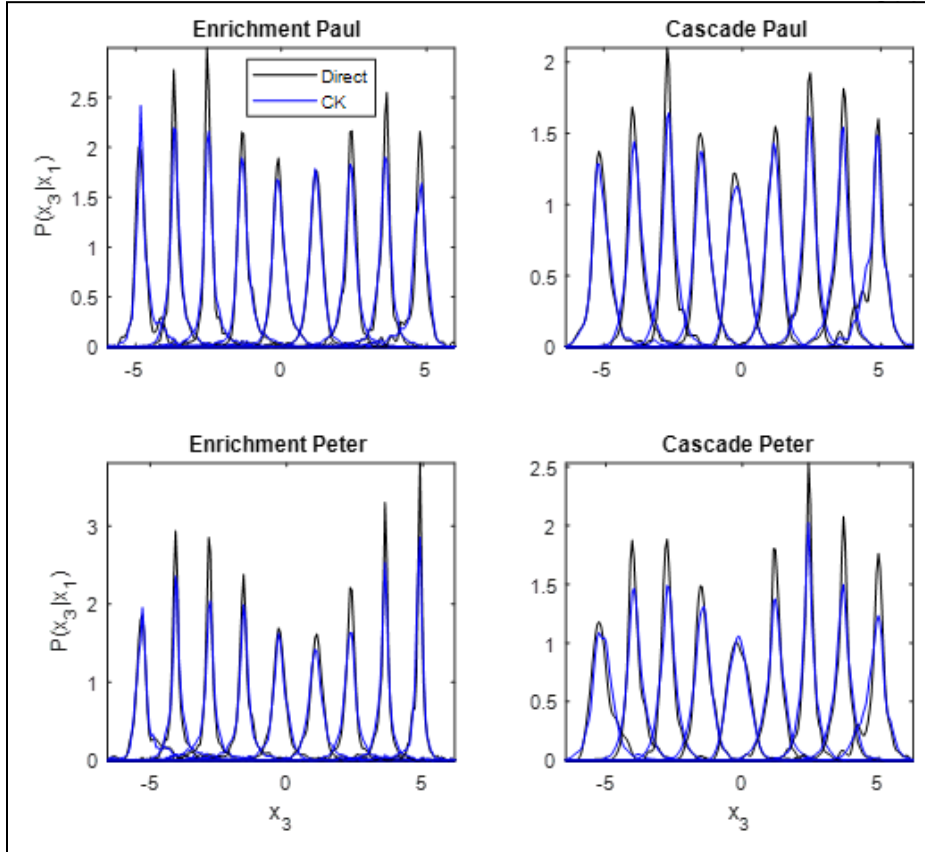
329

Model Validation

331   For each lake in each experiment we compared the observed Langevin model to a hypothetical
332   model with constant drift (the mean of the observed drift) using the negative log likelihoods
333   calculated from the one-step model predictions and observations. In all cases the differences in
334   negative log likelihood (observed model – constant drift model) were negative, indicating a
335   better for the observed model. Differences in negative log likelihood for Peter Lake were -17.55
336   in the Cascade experiment and -6.8 in the Enrichment experiment. In Paul Lake the differences
337   in negative log likelihood were -5.3 in the Cascade experiment and -0.5 in the Enrichment
338   experiment.

339   To illustrate the correspondence of predictions to observations, we compared the one-step-ahead
340   predicted distributions p(x(t+1)|x(t)) from the Langevin equation with the observed one-step

341   ahead dynamics of the pigments. Here x(t) is the standardized level of pigment at one point in
342   time. Comparisons were made for each lake in each experiment at 9 quantiles of the frequency
343   distribution of pigment standardized levels.

344   For the data, we found the corresponding bin for each quartile and then found all pigment values
345   x(t) within this bin. For each x(t) we also found the corresponding observation in the next time
346   step, x(t+1). From these we calculated the distribution of next time step points x(t+1), which is
347   the observed density of next time step points x(t+1) conditioned on the current time step points
348   x(t), i.e., $P(x_{t+1}|x_{t})$. Using the model, we calculated $P(x_{t+1}|x_{t})$ from the Langevin
349   equation with terms estimated from the data.

350   Comparison of the observed and modeled one-step distributions are presented in Fig. S-7.
351   Predicted distributions tightly overlapped with observed distributions.

352

353   Figure S-7. Observed (black) and predicted (blue) one-step probability distributions for 9
354   quartiles of pigment standard level in each lake in each experiment.
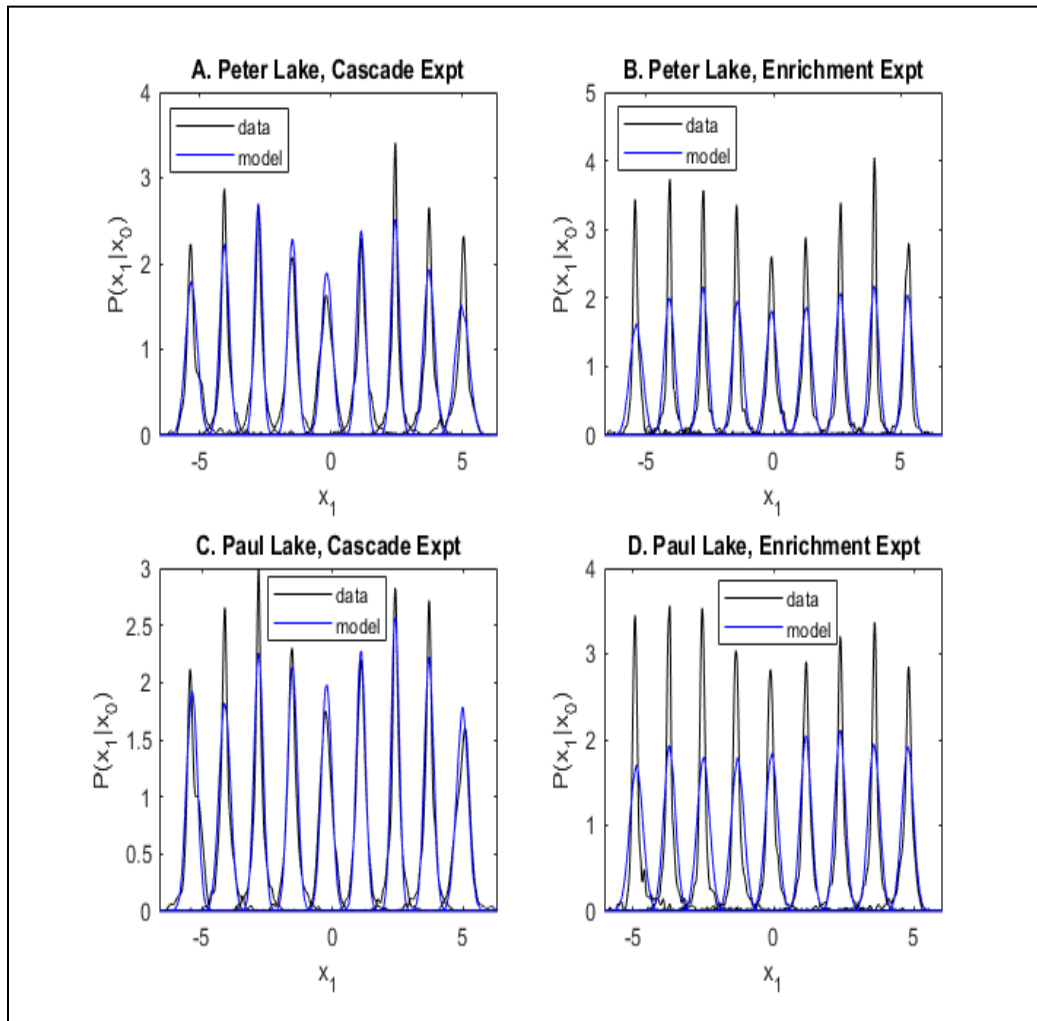
372 *Bootstrapped Uncertainties for the Equilibria*

373 Figure S-6. Bootstrap estimates of uncertainties for the 3 equilibria in Peter Lake for the Cascade
374 experiment (top row, standardized level of chlorophyll *a*) and enrichment experiment (bottom
375 row, standardized level of phycocyanin). Vertical dashed lines show equilibria of the original
376 data.

377
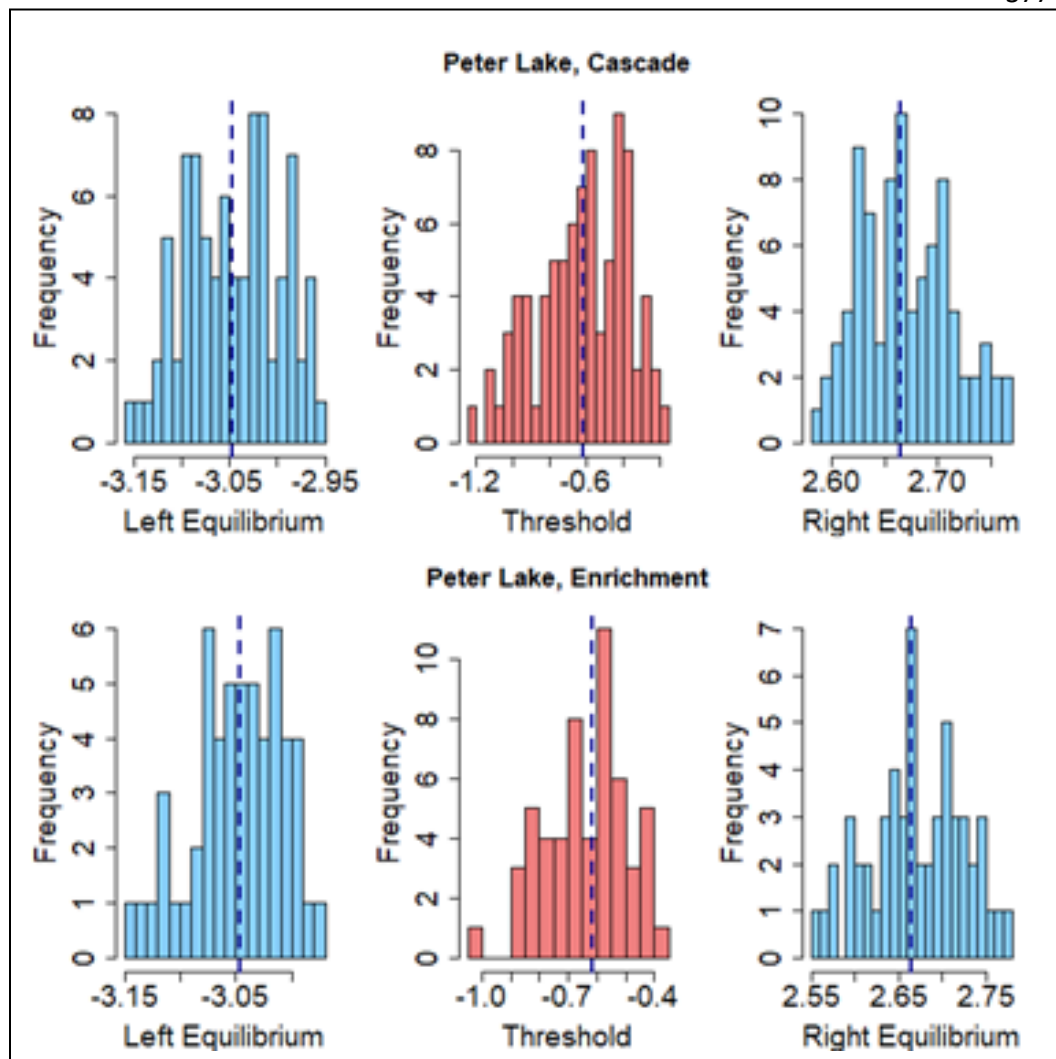
390 Figure S-7. Bootstrap estimates of uncertainties for the 3 equilibria in Paul Lake for the Cascade
391 experiment (top row, standardized level of chlorophyll *a*) and enrichment experiment (bottom
392 row, standardized level of phycocyanin). Vertical dashed lines show equilibria of the original
393 data.

394

413

414

415

416

417

418

419

420
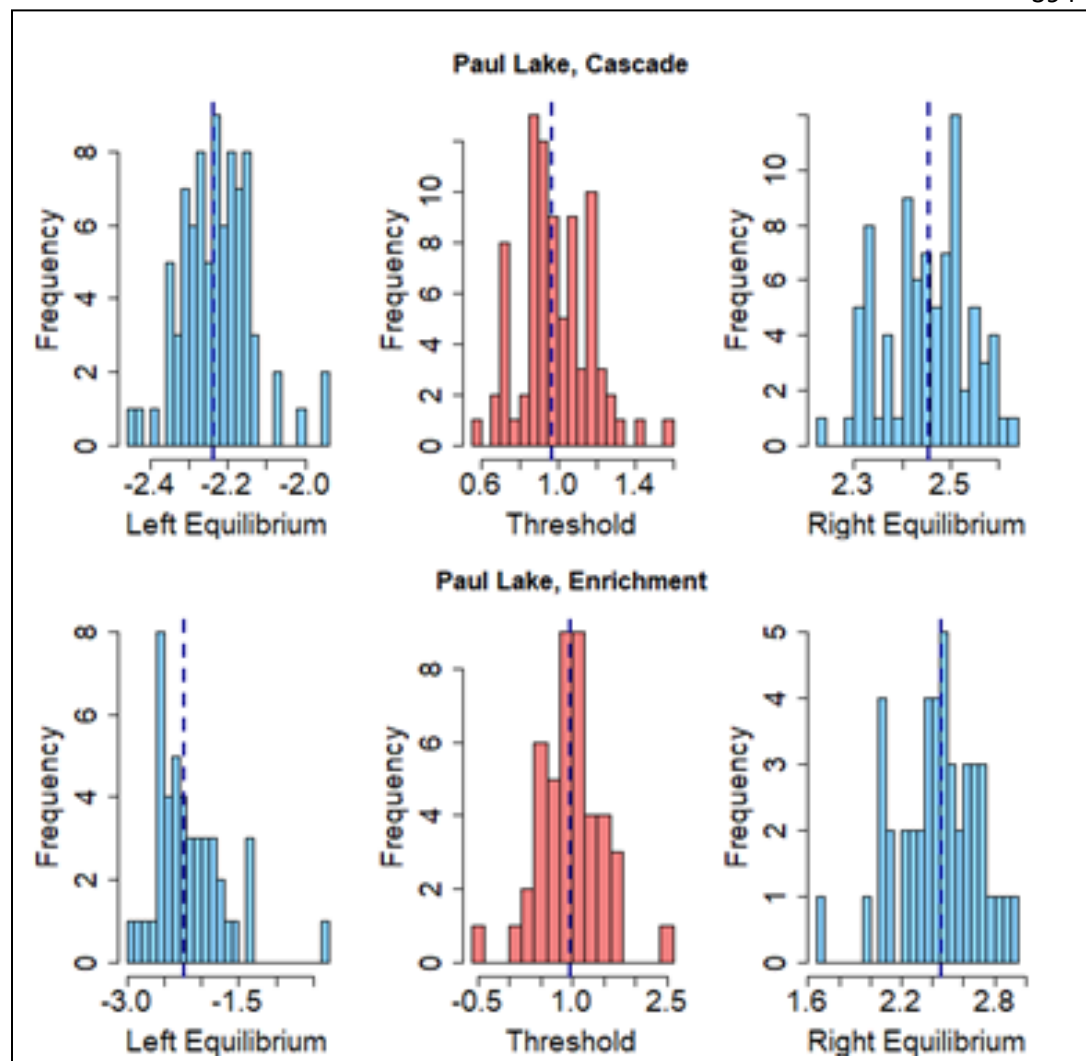
421 *Bootstrapped Uncertainties for Exit Time*

422 Figure S-8. Bootstrap estimates of uncertainty of exit time of Peter Lake for the Cascade (top
423 row) and Eutrophication (bottom row) experiments, for the low-pigment (left column) and high-
424 pigment (right column) basins observed in each experiment. Vertical dashed line shows the
425 estimate from the original data.

426
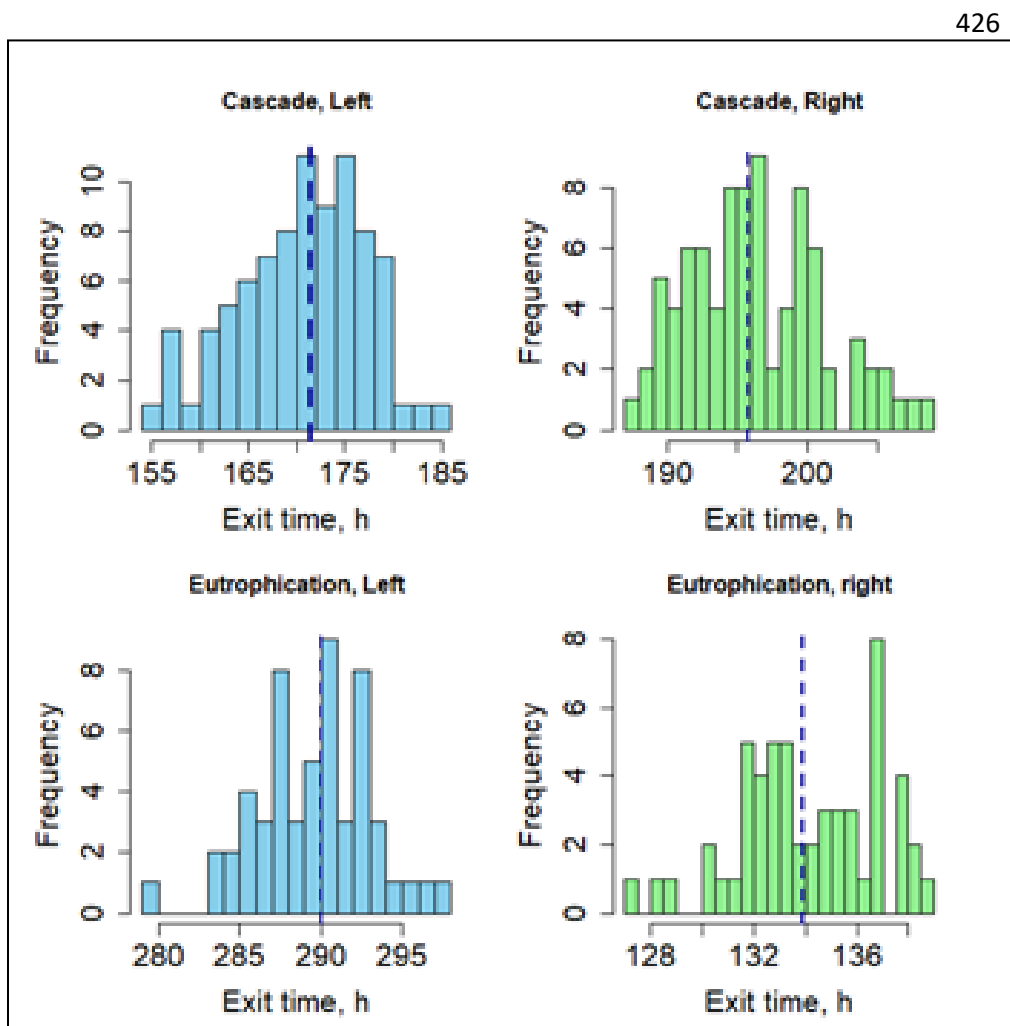

444

445

446

447

448

449

450

Figure S-9. Bootstrap estimates of uncertainty of exit time in the reference ecosystem, Paul Lake, for the Cascade (top row) and Eutrophication (bottom row) experiments, for the low-pigment (left column) and high-pigment (right column) basins observed in each experiment. Vertical dashed line shows the estimate from the original data.

451

471

472

473

474

475

476

477

478

479

480

481
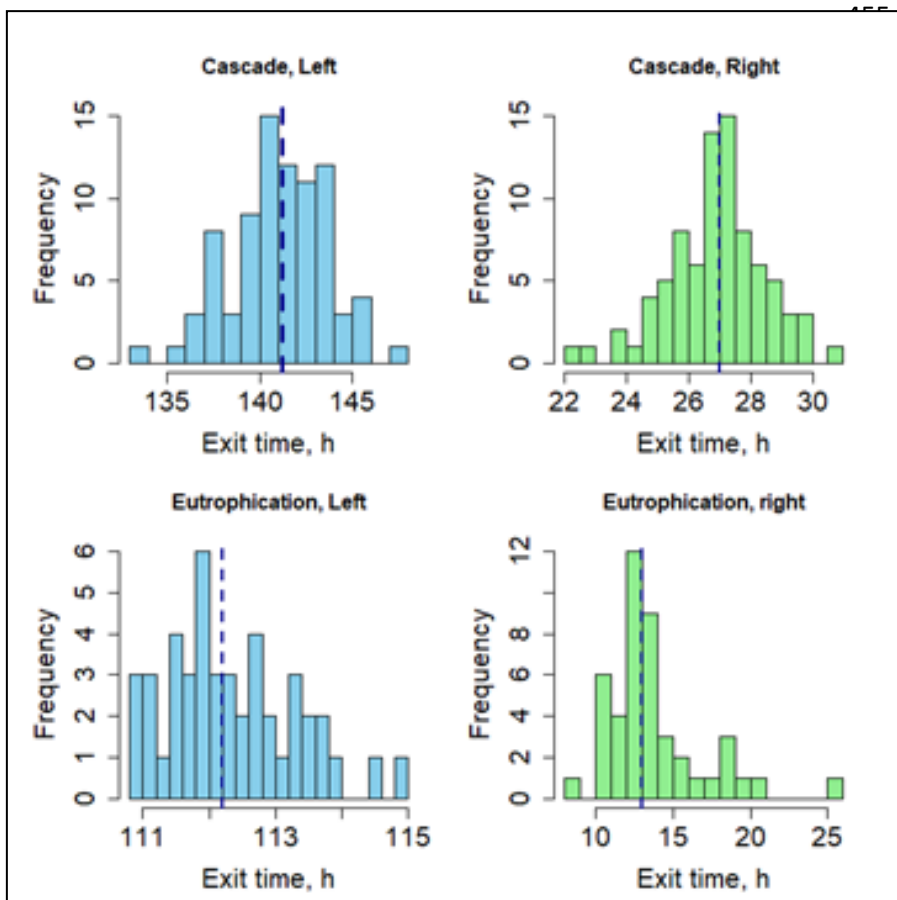
Could Alternate States be Detected by Chance?

We generated phase randomized surrogate time series to show whether we can get alternative
stable states by chance. When our time series are randomized using the Ebisuzaki method using
the surrogates() function in the R library "astrochron" we always get a model with a linear drift
function D1 (implying one stable state) and additive noise (i.e. D2 has no apparent change or
trend with state) (Figure S10). This is not useful for bootstrapped estimates of uncertainty of the
mean exit time, but it does show that we are not likely to see alternate states by chance.

Figure S10. D1 and D2 from 100 pseudodata series from Peter Lake, Enrichment experiment,
bootstrapped by the Ebisuzaki method. In each plot, solid line is the median of the 100 bootstraps
for each state value and the dotted lines are the 10th and 90th quantiles.

Alternate States in Daily Chlorophyll Time Series
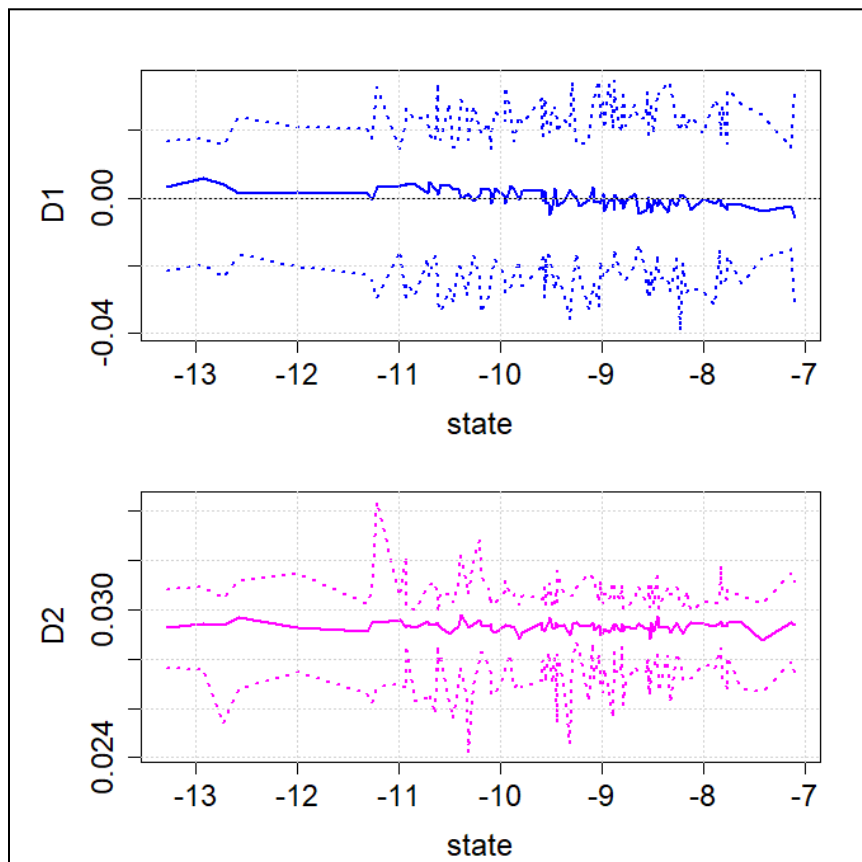
495 Alternate States in Daily Chlorophyll Time Series

496 We considered the possibility that alternate states in Paul Lake were related to variability of
497 sonde data or events of short duration. To check this possibility we analyzed daily chlorophyll
498 samples collected from both lakes on each day of the Cascade and Enrichment experiments.
499 Chlorophyll sampling was conducted throughout the period of summer stratification each year.
500 Water samples from a depth of 0.5 m were collected over the deepest point in the lake each day.
501 During the enrichment experiment water was collected before nutrient additions. The water was
502 filtered through Whatman 47 mm GF/F filters and extracts from the filters were analyzed
503 fluorometrically for chlorophyll a concentration corrected for pheopigments (Holm-Hanson
504 1978).

505 Daily chlorophyll time series were fitted to time-varying autoregressions (eq. S-1) and the level
506 time series b_t (chlorophyll a in µg/L) was used to estimate drift and diffusion. Because of the
507 long time step (1 day) and small sample size (460 intervals), we did not test the effects of longer
508 time lags.

509 Chlorophyll time series in Paul Lake have only one equilibrium, the single root of the drift
510 function (Fig. S9). In the enrichment experiment, the drift function comes close to the zero line
511 at high chlorophyll levels but does not cross the zero line.

512 Chlorophyll time series from both experiments in Peter Lake have three equilibria, indicating
513 two alternate states separated by an unstable threshold (Fig. S10).
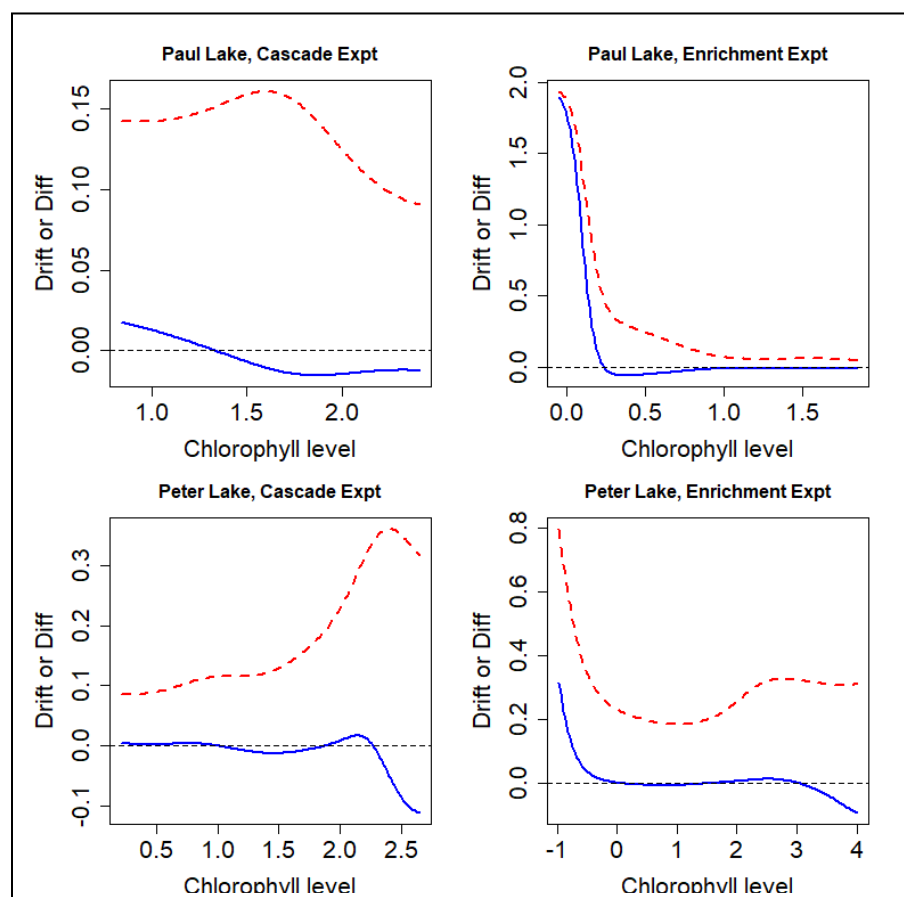

Figure S11. Drift (blue solid line) and diffusion (red dashed line) functions versus chlorophyll a level (µg/L) in Paul Lake, Cascade and Enrichment experiments. Dotted horizontal line at zero.

533   The daily datasets and metadata are available online:

534   Carpenter, S.R., M. Pace, J. Cole, J.F. Kitchell, and J. Hodgson. 2019. Cascade project at North
535   Temperate Lakes LTER - Daily data for key variables in whole lake experiments on early
536   warnings of critical transitions, Paul and Peter Lakes, 2008-2011 ver 1. Environmental Data
537   Initiative. https://doi.org/10.6073/pasta/b0448233e215a969eb5623434fcd4494. Accessed 2021-
538   01-01.

539   Pace, M., J. Cole, and S. Carpenter. 2020. Cascade project at North Temperate Lakes LTER -
540   Daily Chlorophyll Data for Whole Lake Nutrient Additions 2013-2015 ver 2. Environmental
541   Data Initiative. https://doi.org/10.6073/pasta/d480f53082da7ea53e349183a0c8a714. Accessed
542   2021-01-01.

543

544   *References*

545   Arani, B. M. S., S. R. Carpenter, L. Lahti, E. H. van Nes, and M. Scheffer. 2021b. Exit time as a measure of
546   ecological resilience. Science **372**: eaay4895.
547   Carpenter, S. R., B. M. S. Arani, P. C. Hanson, M. Scheffer, E. H. Stanley, and E. Van Nes. 2020. Stochastic
548   dynamics of Cyanobacteria in long-term high-frequency observations of a eutrophic lake.
549   Limnology and Oceanography Letters **5**: 331-336.
550   Friedrich, R., J. Peinke, M. Sahimi, and M. Reza Rahimi Tabar. 2011. Approaching complexity by
551   stochastic methods: From biological systems to turbulence. Physics Reports **506**: 87-162.
552   Hassanibesheli, F., N. Boers, and J. Kurths. 2020. Reconstructing complex system dynamics from time
553   series: a method comparison. New Journal of Physics **22**: 073053.
554   Holm-Hanson, O. 1978. Chlorophyll a determination: improvements in methodology. Oikos **30**: 438-447.
555   Ives, A. R., and V. Dakos. 2012. Detecting dynamical changes in nonlinear time series using locally linear
556   state-space models. Ecosphere **3**: art58.
557   May, R. M. 1977. Thresholds and breakpoints in ecosystems with a multiplicity of stable states. Nature
558   **269**: 471-477.
559   Pole, A., M. West, and J. Harrison. 1994. Applied Bayesian forecasting and time series analysis. Chapman
560   & Hall.
561   Tabar, M. R. R. 2019. Analysis and Data-Based Reconstruction of Complex Nonlinear Dynamical Systems.
562   Springer Nature.
563   West, M., and P. J. Harrison. 1989. Bayesian Forecasting and Dynamic Models. Springer-Verlag.

564